NASA TECHNICAL MEMORANDUM

NASA TM X-1846

NASA TM X-1846

Corrected Copy

DESIGN STUDIES ON THE EFFECTS OF ORIENTATION, LUNATION, AND LOCATION ON THE PERFORMANCE OF LUNAR RADIATORS

by Thomas Dallas, Anthony J. Diaguila, and James F. Saltsman

Lewis Research Center
Cleveland, Ohio 44135

NATIONAL AERONAUTICS AND SPACE ADMINISTRATION • WASHINGTON, D. C. • MARCH 1971

1. Report No. NASA TM X-1846	2. Government Accession No.	3. Recipient's Catalog No.
4. Title and Subtitle DESIGN STUDIES ON THE EFFECTS OF ORIENTATION, LUNATION, AND LOCATION ON THE PERFORMANCE OF LUNAR RADIATORS		5. Report Date March 1971
		6. Performing Organization Code
7. Author(s) Thomas Dallas, Anthony J. Diaguila, and James F. Saltsman		8. Performing Organization Report No. E-4570
9. Performing Organization Name and Address Lewis Research Center National Aeronautics and Space Administration Cleveland, Ohio 44135		10. Work Unit No. 120-27
		11. Contract or Grant No.
		13. Type of Report and Period Covered Technical Memorandum
12. Sponsoring Agency Name and Address National Aeronautics and Space Administration Washington, D.C. 20546		14. Sponsoring Agency Code

15. Supplementary Notes

Corrected copy

16. Abstract

This report permits a rapid approximate estimate of the effective sink temperature and of the size of a waste-heat-rejection radiator for a lunar thermodynamic system whether for refrigeration, power generation or component cooling. An included problem for a 500-kilowatt power generation system gives 4600 and 6000 square feet for a polar and for an equatorial location, respectively.

17. Key Words (Suggested by Author(s))	18. Distribution Statement
Lunar radiator	Unclassified - unlimited

19. Security Classif. (of this report)	20. Security Classif. (of this page)	21. No. of Pages	22. Price*
Unclassified	Unclassified	41	$3.00

*For sale by the National Technical Information Service, Springfield, Virginia 22151

DESIGN STUDIES ON THE EFFECTS OF ORIENTATION, LUNATION, AND LOCATION ON THE PERFORMANCE OF LUNAR RADIATORS

by Thomas Dallas, Anthony J. Diaguila, and James F. Saltsman

Lewis Research Center

SUMMARY

The performance of lunar radiators was studied for various radiator orientations (with respect to the lunar surface and the Sun), lunar day and night conditions, and location.

The vertical radiator with two active sides had a higher heat-rejection rate than the horizontal radiator of the same overall dimensions with one active side. Direct solar radiation has little effect on the performance if the solar absorptance can be made small (about 0.20 or less) for low radiator temperatures (about 760° R or 422 K). For higher radiator temperatures (1460° R or 811 K), solar radiation effects remain small, even with solar absorptance values of 0.75.

For low-temperature cooling requirements, a horizontal radiative surface is essential. A radiator in polar location would be appreciably smaller because the Moon surface is colder and there is no sunshine.

Graphical solutions of the design equations are presented. This expedites the procedure for approximating prime radiator areas for preliminary studies of lunar heat-rejection systems. The effective sink temperature for any given set of radiator conditions is readily obtained from equations and graphs are presented.

INTRODUCTION

In space, heat can be rejected from a system only by radiant heat transfer. For this reason, a space radiator might be quite large unless high radiating temperatures can be used. Large areas plus additional material required for meteoroid protection result in heavy waste-heat-rejection systems.

The sizes of space radiators, whether they are for heat-rejection systems of a space or lunar power plant, for cooling of the power plant components, or for refrigeration systems, are basically determined by the amount of heat they must reject, temperature of the radiator surface, and the effective sink temperature. The radiator temperature is essentially determined by thermodynamic cycle efficiency, pumping fluid characteristics, and allowable material temperatures. In lunar radiators; the effective sink temperature is influenced by the orientation of the radiator surface with respect to the Sun and the surface of the Moon, as well as daytime and nighttime conditions and radiator location. The performance of a radiator is improved by lower sink temperatures which results in smaller radiator areas.

Design analyses for space and lunar power systems have shown that the waste-heat radiators for these systems are, in many cases, the heaviest components in the complete power system. This study analyzed the effects of radiator orientation, location, and lunation on the heat-rejection capabilities of lunar radiators.

Heat-rejection rates of a radiator operating over a complete lunation (which is the interval from one new moon to the next) are presented for three specific cases:

Case A - Radiating surface flat on the equator of the Moon with solar radiation incident on its surface. The side facing the Moon is insulated.

Case B - Radiating surface upright on the equator of the Moon with solar radiation incident on its surface. The plane of the radiator is normal to the plane of the ecliptic.

Case C - Radiating surface upright on the equator of the Moon with no solar radiation incident on its surface. The radiator surface is in the plane of the ecliptic.

The coolant temperature range considered in the analyses of these three radiators is at the level encountered when considering the waste-heat radiators for lunar-based power-plant systems presently being considered. The range also covers component coolant loops for these systems, as well as refrigeration system condensing radiators. In the calculations given in this report, the coolant temperature range is from 560° to 1660° R (311 to 922 K). The basic heat-rejection data are presented for a complete lunation for a range of average radiator surface temperatures and the corresponding surface heat-transfer characteristics (ϵ and α_s).

Graphical solutions for equations which convert representative fluid inlet and outlet temperatures to average radiator surface temperatures are also presented. These graphs enhance the usefulness of the information presented herein for approximating radiator areas for various lunar applications.

It must be noted that in this analysis the heat-transfer area is the prime area. An example of prime radiator area would be the two large flat surfaces on a thin rectangular duct in which the heat-rejection fluid is flowing and which have an unobstructed view of the heat sink. In other constructions a multiplication factor including fin effectiveness and interradiation effects, which are dependent on the specific geometry of the radiator, is required in order to obtain actual radiator areas.

METHOD OF ANALYSIS

Heat-Rejection Equations

In the discussion that follows, in order to illustrate the advantage of a vertical radiator over a horizontal radiator, which necessarily has one insulated surface, q will be the heat-rejection flow rate of a 1- by 1-foot (0.305- by 0.305-m) section of radiator regardless of whether it has one or two active sides. The symbol A_R, represents the number of these 1- by 1-foot (0.305- by 0.305-m) radiator sections, and A_R, will represent the actual radiating surface in square feet. In the case of a 1- by 1-foot (0.305- by 0.305-m) section, A_R for a vertical radiator would be 2 square feet (0.186 m^2), and for a horizontal radiator 1 square foot (0.093 m^2). In both cases only prime radiator area or size is considered.

The rate of heat rejection by the radiator is given by the following equation:

$$Q = wC_p(T_{fi} - T_{fo}) \tag{1}$$

(All symbols used in this report are defined in appendix A.)

The prime radiating surface area required for a radiator to reject a given amount of heat is determined by the equation (see ref. 1).

$$A'_R = wC_p\left\{\frac{1}{h_R}\ln\frac{T_{wi}^4 - T_s^4}{T_{wo}^4 - T_s^4} + \frac{1}{4\sigma\epsilon T_s^3}\left[\ln\frac{(T_{wi} - T_s)(T_{wo} + T_s)}{(T_{wo} - T_s)(T_{wi} + T_s)} - 2\left(\arctan\frac{T_{wi}}{T_s} - \arctan\frac{T_{wo}}{T_s}\right)\right]\right\} \tag{2}$$

If equation (1) is divided by equation (2), the radiator heat flow per unit area is obtained.

$$\frac{Q}{A'_R} = \frac{T_{fi} - T_{fo}}{\frac{1}{h_R}\ln\frac{T_{wi}^4 - T_s^4}{T_{wo}^4 - T_s^4} + \frac{1}{4\sigma\epsilon T_s^3}\left[\ln\frac{(T_{wi} - T_s)(T_{wo} + T_s)}{(T_{wo} - T_s)(T_{wi} + T_s)} - 2\left(\arctan\frac{T_{wi}}{T_s} - \arctan\frac{T_{wo}}{T_s}\right)\right]} \tag{3}$$

The fluid temperatures T_{fi} and T_{fo} are normally the initial parameters computed for the radiator. The relations between these temperatures and the radiator wall temperatures T_{wi} and T_{wo} can be obtained by taking a heat balance at any location on the radiator. The heat balance is made between the radiative and convective heat flow for a unit area. The temperature drop through the wall is assumed to be small. Therefore, the outside wall temperature is approximately equal to the inside wall temperature. Equating the convective and the radiative heat flow results in the following expression:

$$h_R(T_f - T_w) = \sigma\epsilon\left(T_w^4 - T_s^4\right) \tag{4}$$

Rearranging this equation gives the general expression for the wall temperature

$$T_w = T_f - \frac{\sigma\epsilon}{h_R}\left(T_w^4 - T_s^4\right) \tag{5}$$

For the radiator inlet equation (5) becomes

$$T_{wi} = T_{fi} - \frac{\sigma\epsilon}{h_R}\left(T_{wi}^4 - T_s^4\right) \tag{6}$$

For the radiator outlet equation (5) becomes

$$T_{wo} = T_{fo} - \frac{\sigma\epsilon}{h_R}\left(T_{wo}^4 - T_s^4\right) \tag{7}$$

In the equations (4) to (7) the radiator surface emittance ϵ and the convection heat-transfer coefficient h_R can usually be estimated. The effective sink temperature can be calculated as shown in the next section.

Effective Sink Temperature

Lunation, radiator location, and orientation are the variables that affect the sink temperature T_s of the radiator. The radiator sees three different sinks: (1) the surface of the Moon, which is assumed to be black body, (2) space, and (3) the Sun. For this reason equations must be developed expressing the effective sink temperature T_s as a function of the preceding variables. The heat-rejection rate for a 1- by 1-foot (0.305- by

0.305-m) section of radiator with one active side can be expressed in terms of radiator orientation, location, and lunation as

$$q = \epsilon\sigma T_{w,av}^4 - F_1\epsilon\sigma T_M^4 - \left|G_s\alpha_s \cos\theta_n\right| \tag{8}$$

The Moon's temperature T_M is given in figure 1. The term G_s is the solar con-

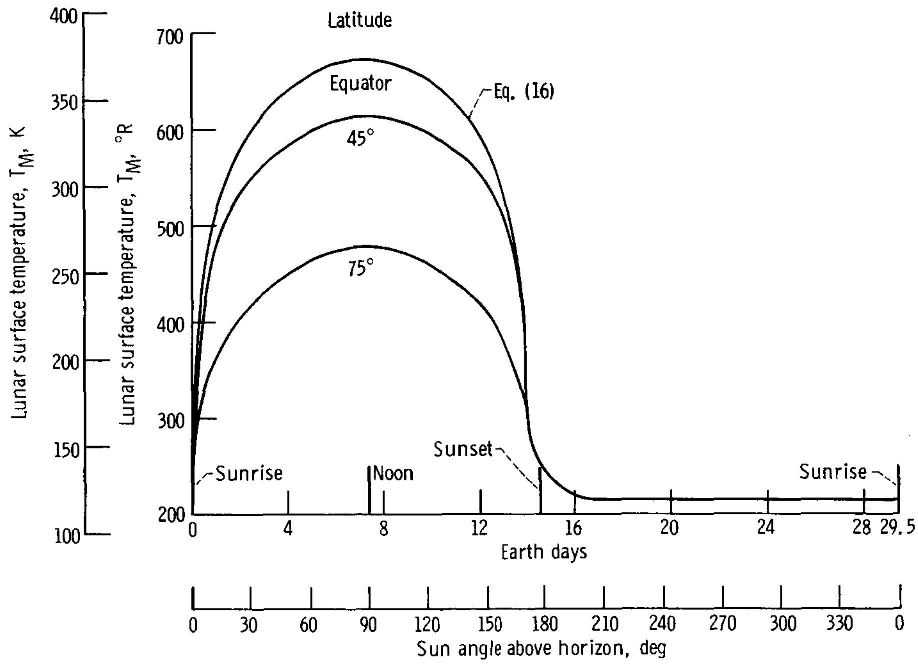

Figure 1. - Lunar surface temperature.

stant, and α_s is the solar absorptance of the radiator surface. The angle of incidence of the Sun is accounted for by θ_n (see fig. 2). Equation (8) as stated above is for one active side and is given in reference 2. The view factor F_1 is for the active side and is given in reference 3. The Moon's albedo is neglected because it is considered a black body (see appendix B). The effect of the presence of the radiator on the Moon's surface temperature is neglected, also.

If the radiator has two active sides, the heat-rejection equation becomes

$$q = 2\epsilon\sigma T_{w,av}^4 - F_1\epsilon\sigma T_M^4 - F_2\epsilon\sigma T_M^4 - \left|G_s\alpha_s \cos\theta_n\right| \tag{9}$$

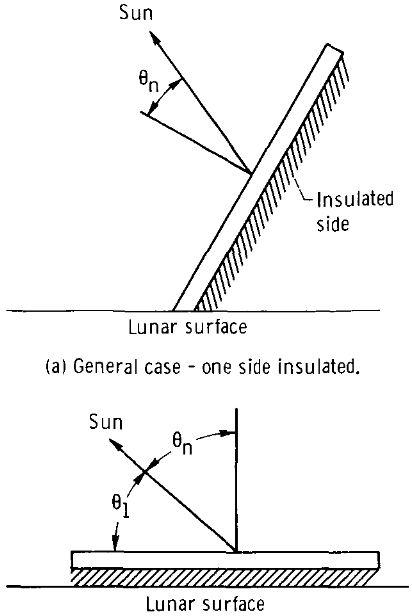

(a) General case - one side insulated.

(b) Case A - horizontal radiator.

Figure 2. - Orientation of radiator on surface of Moon.

But $F_1 + F_2 = 1.0$, so equation (9) becomes

$$q = 2\epsilon\sigma T_{w,av}^4 - \epsilon\sigma T_M^4 - \left|G_s \alpha_s \cos\theta_n\right| \tag{10}$$

The radiator average wall temperature $T_{w,av}$ in these equations is the integrated average of the temperature of the radiator surfaces. The method of determining this will be given in a later section.

The heat-rejection rate for a 1- by 1-foot (0.305- by 0.305-m) section of a radiator with one active side can be expressed in terms of average wall and sink temperature by the following equation (The right side of equation (11) happens to be the heat-rejection rate per unit prime area, also):

$$q = \epsilon\sigma\left(T_{w,av}^4 - T_s^4\right) \tag{11}$$

And, if the radiator has two active sides, the right side of equation (11) must be multiplied by 2.0.

An expression for effective sink temperature for a radiator with one active side, can be found by combining equations (8) and (11).

$$\epsilon\sigma T^4_{w,av} - F_1\epsilon\sigma T^4_M - \left|G_s\alpha_s \cos\theta_n\right| = \epsilon\sigma\left(T^4_{w,av} - T^4_s\right) \tag{12}$$

Solving for the effective sink temperature yields

$$T_s = \left[F_1 T^4_M + \left|\frac{G_s}{\sigma}\left(\frac{\alpha_s}{\epsilon}\right)\cos\theta_n\right|\right]^{1/4} \tag{13}$$

For a radiator with two active sides, equation (10) is combined with equation (11). Note that equation (11) must be multiplied by 2.0 because there are two active sides.

$$2\epsilon\sigma T^4_{w,av} - \epsilon\sigma T^4_M - \left|G_s\alpha_s \cos\theta_n\right| = 2\epsilon\sigma\left(T^4_{w,av} - T^4_s\right) \tag{14}$$

Solving for T_s results in

$$T_s = \left[\frac{T^4_M}{2} + \left|\frac{G_s}{2\sigma}\left(\frac{\alpha_s}{\epsilon}\right)\cos\theta_n\right|\right]^{1/4} \tag{15}$$

In the equation for T_s, the surface temperature of the Moon T_M at various locations can be obtained from figure 1. These data were taken from reference 4. The numerical value of the solar constant G_s of 430 Btu/(hr)(ft^2) (1.356 kW/m^2) used in the calculations herein was taken from references 4 (pp. 7-9) and 5 (p. 236).

The value of the temperature of the Moon at its equator can also be obtained from equation (16) for the interval from sunrise to sunset (ref. 2). In the equation, D_a is Earth days, the argument of the sine is in degrees, and the temperature is in degrees Rankine (to get degrees Kelvin the factor 5/9 must be used).

$$T_M = 673 \sin^{1/6}\left(\frac{90\ D_a}{7}\right) \tag{16}$$

Radiator Average Wall Temperature

In a section to follow, an alternate procedure for calculating radiator size is given in terms of $T_{w,av}$. This procedure uses a form of equation (11), which was presented in the development of the sink temperature equations. The inputs to this equation are essentially T_s and $T_{w,av}$. Equations for T_s were developed previously. An expression for $T_{w,av}$ will follow.

It should also be noted that equation (11) is used as the basic equation in the analyses of the performance of the radiator. The performance can be more clearly presented with this equation using $T_{w,av}$ and T_s rather than equation (3).

When the heat-rejection process is one similar to condensing, the fluid temperature is uniform and nearly constant from inlet to exit conditions. For this case, the arithmetic average of the inlet and exit wall temperatures can be used for $T_{w,av}$. However, in a radiator, the temperature of the fluid decreases from inlet to outlet so that an integrated average should be used for this case.

The expression for the radiator average wall temperature can be developed using a modified form of equation (11). If both sides of equation (11) are multiplied by A'_R an expression for the rejected heat flow rate is obtained.

$$Q = \epsilon\sigma A'_R\left(T^4_{w,av} - T^4_s\right) \tag{17}$$

Solving equation (17) for $T_{w,av}$ gives

$$T_{w,av} = \left(\frac{1}{\epsilon\sigma}\frac{Q}{A'_R} + T^4_s\right)^{1/4} \tag{18}$$

Substituting equation (3) into equation (18) gives the following expression for $T_{w,av}$:

$$T_{w,av} = \left[\frac{T_{fi} - T_{fo}}{\epsilon\sigma\left\{\frac{1}{h_R}\ln\frac{T^4_{wi} - T^4_s}{T^4_{wo} - T^4_s} + \frac{1}{4\sigma\epsilon T^3_s}\left[\ln\frac{(T_{wi} - T_s)(T_{wo} + T_s)}{(T_{wo} - T_s)(T_{wi} + T_s)} - 2\left(\arctan\frac{T_{wi}}{T_s} - \arctan\frac{T_{wo}}{T_s}\right)\right]\right\}} + T^4_s\right]^{1/4} \tag{19}$$

If equations (6) and (7) are solved for T_{fi} and T_{fo}, respectively, and substituted into equation (19) the following expression is formed:

$$T_{w,av} = \left[\frac{T_{wi} - T_{wo} + \frac{\epsilon\sigma}{h_R}\left(T^4_{wi} - T^4_{wo}\right)}{\epsilon\sigma\left\{\frac{1}{h_R}\ln\frac{T^4_{wi} - T^4_s}{T^4_{wo} - T^4_s} + \frac{1}{4\epsilon\sigma T^3_s}\left[\ln\frac{(T_{wi} - T_s)(T_{wo} + T_s)}{(T_{wo} - T_s)(T_{wi} + T_s)} - 2\left(\arctan\frac{T_{wi}}{T_s} - \arctan\frac{T_{wo}}{T_s}\right)\right]\right\}} + T^4_s\right]^{1/4} \tag{20}$$

The calculation of $T_{w,av}$ from this equation is not straightforward. For this analysis, equation (20) was plotted with the quantity $T_{wi} - T_{wo}$ as the independent variable and with the quantity T_{wo} as the parameter. The emittance ϵ, film coefficient h_R, and the sink temperature T_s, are held constant for a particular family of curves. A typical set of curves will be presented in the section Lunar Radiator Design Curves.

Specific Design Equations

The basic variable for the cases analyzed in this report is the effective sink temperature T_s. The general expression for this temperature was given previously (eqs. (13) and (15)). The following equations are for the three specific cases considered.

Case A - horizontal position. - For this case the radiator is lying flat on the surface of the Moon. The bottom side is thermally insulated from the surface. Thus, there is only one active side, and equation (13) applies. Since the active side of the radiator does not see the Moon's surface, $F_1 = 0$ and $\cos\theta_n$ can be replaced by $\sin\theta_1$, where θ_1 is the angle of the Sun above the horizon (see fig. 2).

Thus, for this particular case equation (13) reduces to

$$T_s = \left[\frac{G_s}{\sigma}\left(\frac{\alpha_s}{\epsilon}\right)\sin\theta_1\right]^{1/4} \tag{21}$$

Case B - vertical radiator, solar energy incident. - For this case the radiator is normal to the Moon's surface. It is also in a plane normal to the plane of the ecliptic. There are two active sides, so equation (15) gives T_s for this case

$$T_s = \left[\frac{T_M^4}{2} + \left|\frac{G_s}{2\sigma}\left(\frac{\alpha_s}{\epsilon}\right)\cos\theta_n\right|\right]^{1/4} \tag{15}$$

Case C - vertical radiator, no solar energy incident. - For this case the radiator is normal to the Moon's surface. But is is essentially in the same plane as the ecliptic. Note that these conditions can be met only on the equator. There are two active sides, and the solar contribution is zero. Thus equation (15) becomes

$$T_s = \frac{T_M}{1.189} \tag{22}$$

As noted previously, T_M can be taken from figure 1 or equation (16) may be used.

It should be noted that in all three cases the radiators are at the equator, but appendix B discusses how to handle a radiator problem for a polar location.

Design Procedures

An approach that can be used in sizing a lunar radiator with the analysis presented is to use equation (2). The temperatures T_{wi} and T_{wo} can be determined from known fluid temperatures and combined with appropriate values of T_s, ϵ, α_s, h_R, C_p and fluid flow rate to determine prime radiator area. The effective sink temperatures T_s can be for a specific lunar time or vary over a lunation.

Another approach for calculating radiator sizes is to use the expressions containing average wall temperature developed in the previous section. The procedure for this approach follows.

The value of q is expressed in equation (11) as

$$q = \epsilon\sigma\left(T_{w,av}^4 - T_s^4\right) \tag{11}$$

The radiator average wall temperature $T_{w,av}$ is found using equation (20), and the effective sink temperature T_s is found using equations (15), (21), or (22). The radiator wall inlet T_{wi} and outlet T_{wo} temperatures (needed in eq. (20)) are determined by equations (6) and (7), respectively, from the known fluid temperatures T_{fi} and T_{fo}. The form of these equations suggests that plotting T_{fi} (or T_{fo}) for assumed values of T_{wi} (or T_{wo}) is the easiest way of determining T_{wi} (and T_{wo}) for given values of h_R, ϵ, and T_s.

After q is determined (eq. (11)), the prime radiator size A_R can be calculated using the following equation (The radiator may have either one or two active sides):

$$A_R = \frac{Q}{q} \tag{23}$$

The design procedure for determining radiator areas using these equations is summarized as follows:

(1) Determine the radiator heat load Q using equation (1) from given values of fluid temperatures, fluid flow rate, and C_p.

(2) Determine the effective sink temperature T_s using the appropriate equation (eqs. (15), (21), or (22); curves may be used if they are available).

(3) Determine T_{wi} and T_{wo} using equations (6) and (7), respectively (curves may be used if they are available).

(4) Determine $T_{w,av}$ using equation (20) (curves may be used if they are available; be illustrated in the sample problem).

(5) Determine q using equation (11) or figure 9 for the specific cases.

(6) Determine A_R using equation (23).

Radiator prime areas can be found after step 3 in this procedure by using equation (2). In order to base the radiator performance on $T_{w,av}$ the additional steps were included.

RESULTS AND DISCUSSION

Performance

Heat-rejection characteristics. - During a complete lunation, the temperature on the surface of the Moon at its equator varies from about 673° R (374 K) at lunar noon to 213° R (118 K) at lunar midnight. This variation decreases as the latitude increases. In the polar region the lunar temperature is essentially constant. The temperature variation along the equator and at various latitudes for a complete lunation is shown in figure 1.

It can be seen from the expressions for q (eqs. (8) and (10)) that the lunar temperature T_M and the radiator average wall temperature $T_{w,av}$ enter these equations to the fourth power. For this reason $T_{w,av}$ and T_M variations may affect the performance of a radiator appreciably. Orientation of the radiator surface also affects the radiant heat interchange between the radiator and the Moon, space, and Sun. The extent of these effects can be demonstrated by examining each component that makes up equation (8). Representative conditions of Moon and radiator temperatures, orientation, and surface radiative heat-transfer characteristics (table I) are substituted in the expression, and the results are presented in table II.

The two radiator surface temperature conditions shown in table II are representative of low and high values (760° and 1460° R; 422 and 811 K) for lunar systems applications. The radiating surfaces are assumed to have coatings with an emmittance ϵ of 0.90 and a solar absorptance α_s of 0.08 and 0.75. The vertical and horizontal radiator positions are considered. In both cases one side of the radiator is insulated.

The first term in equation (8) (table II(a)) is the heat per unit area radiating from the radiator surface. This term varies as the fourth power of the radiator wall temperature. Increasing the temperature from 760° to 1460° R (422.1 and 811.0 K) increases the emission from 514.6 to 7009.1 Btu/(hr)(ft^2) (1.6 and 22.1 W/m^2).

The second term (table II(b) is the heat input into the radiator (per unit area) from the surface of the Moon. This term is also affected by F_1. The effect of the Moon on the

TABLE I. - SOLAR ABSORPTANCE AND EMITTANCE OF POSSIBLE RADIATOR COATINGS

Pigment	Binder	Surface test temperature		Test exposure time, sun hr	Solar absorptance, α_s		Emittance, ϵ	Recommended temperature range		Coating designation	Reference
		^{o}R	K		Initial	Final		^{o}R	K		
Magnesium oxide	---------	530	294.1	-----	0.08	----	0.90	-------	-------	----	5 and 6
Zinc oxide	Potassium silicate	550 955	305 530	1050 7200	.16 .17	0.18 .33	.85 .85	To 960	To 533	Z93	7
Stannic oxide	Cr-Co-Ni spinel	To 1060	To 589	1 yr	.3	.3	.91	To 1060	To 589	AI93	8 and 9
Iron titanate	Co 1-percent Zr	To 2260	To 1255	[a]5000	[b].75	----	.88	To 2260	To 1255	----	10

[a]Cycle tests, 1960^{o} to 2260^{o} R (1090 to 1255 K).

[b]At 1020^{o} R (567 K). Unpublished data from authors of ref. 9.

TABLE II. - EQUATION 8 TERMS COMPRISING LUNAR RADIATOR

HEAT-REJECTION RATE

[Radiator emittance, 0.90; solar absorptance, 0.08 and 0.75.]

(a) First term, surface emission

Average wall temperature, $T_{w,av}$		Surface emission, $\epsilon\sigma T_{w,av}^4$	
^oR	K	Btu/(hr)(ft^2)	kW/m^2
760	422	514.6	1.623
1460	811.0	7009.1	22.107

(b) Second term, lunar heat input

Lunar temperature, T_M		Shape factor, F	Lunar heat input, $F_1\epsilon\sigma T_M^4$	
^oR	K		Btu/(hr)(ft^2)	kW/m^2
673	374	0.50 (Vertical) 0 (Horizontal)	155.48 0	0.4904 0
213	118	0.50 (Vertical) 0 (Horizontal)	1.5876 0	0.005007 0

(c) Third term, solar heat input

Solar included angle, θ_n, deg	Solar absorptance, α_s			
	0.08		0.75	
	Solar heat input, $G_s\alpha_s \cos\theta_n$			
	Btu/(hr)(ft^2)	kW/(m^2)	Btu/(hr)(ft^2)	kW/(m^2)
0	34.4	0.1082	322.5	1.015
90	0	0	0	0

radiator is maximum when the radiator is vertical (F_1 = 0.50) and is zero when the radiator is horizontal (F_1 = 0). The two lunar temperatures presented are for the extreme conditions (lunar noon, 673^o R (374 K); and midnight, 213^o R (118 K)) on the Moon's equator. The variation in the Moon's surface temperature at this location is about 460^o R (256 K). Thus the second term in equation (8) can vary by a factor of about 100 for a vertical radiator on the equator. For a horizontal radiator this term is zero.

As indicated in figure 1, the least variation for this term for a vertical radiator will occur at or near the pole. The lunar surface temperature variation increases with decreasing latitudes.

The third term in equation (8) (table II(c)) is the heat input to the radiator from the Sun. This term is maximum when $\theta_n = 0^o$ and is zero when $\theta_n = 90^o$.

From table I it can be seen that a coating material with α_s of approximately 0.08 may be feasible for a radiator wall temperature of approximately 760° R (422 K), but, for a 1460° R (811 K) material, α_s becomes 0.75. However, comparison of the ratio of direct solar radiation to the radiator surface emission (table II) gives 34.4/514.6 = 6.7 percent and 322.5/7009.1 = 4.6 percent for α_s = 0.08 and 0.75, respectively. These values demonstrate that direct solar heat is a small percentage of the net radiator heat flux and is not a major problem.

Effective sink-temperature variation. - Variation in effective sink temperature during a complete lunation for one horizontal and two vertical radiators is shown in figure 3.

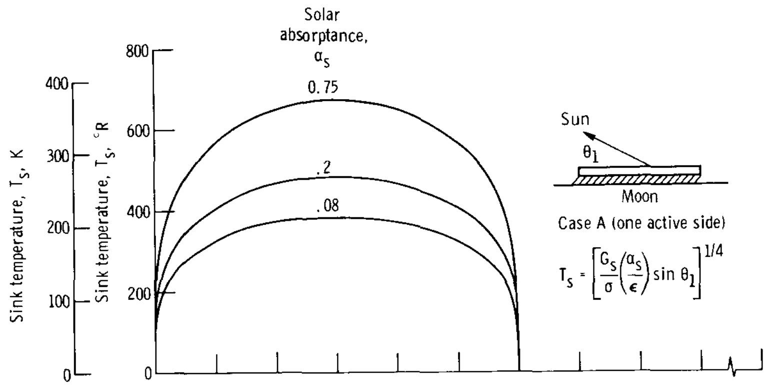

(a) Case A, one active side.

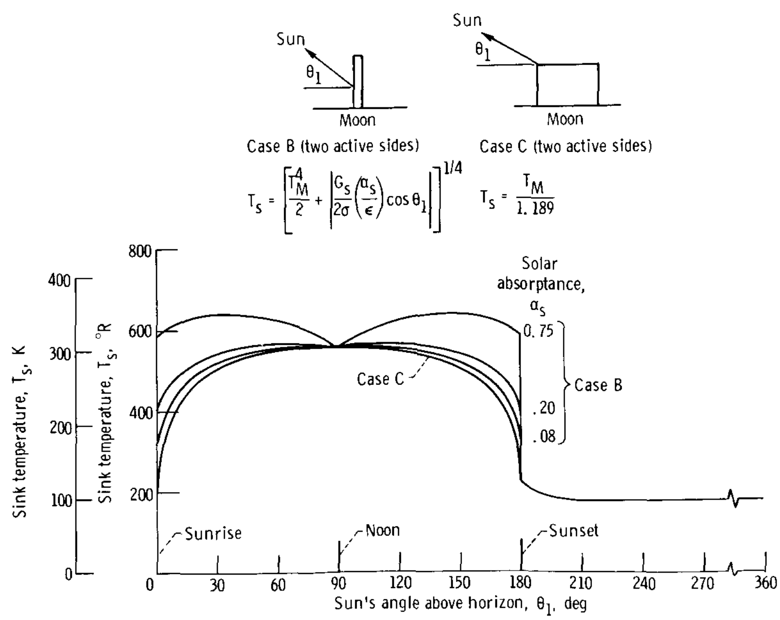

(b) Cases B and C.

Figure 3. - Effective sink temperature for various radiator positions located on equator. Emittance, 0.90.

For the horizontal case the sink temperature ranges from about 675° to 0° R (375.5 to 0 K) for α_s of 0.75. For $\alpha_s = 0.08$, the sink temperature ranges from 386° to 0° R (214 to 0 K).

A comparison of these temperatures for the two upright radiators with and without solar radiation incident on the surface shows only a slight difference in magnitude for low α_s's during the sunrise and sunset hours. At lunar noon, the sink temperature is the same for both upright radiators. For these cases, the sink temperature ranges from about 565° to 180° R (314 to 100.0 K).

The range of fluid temperatures for cooling electronic equipment is from 400° to 570° R (220 to 317 K). Thus a coolant system for such equipment would most likely require a horizontal radiator with a low absorptance coating for operation on the equator over a complete lunation. A vertical radiator will reject heat only during the lunar nighttime for these temperatures.

Figure 1 shows that at the higher latitudes the lunar surface temperature decreases. In the polar regions, minimum surface temperatures exist. Deep craters near the poles have permanent shadows on their floors, so in these areas the temperature is constant and near the minimum lunar surface temperatures of approximately 213° R (118 K) (ref. 4). At these locations minimum radiator areas can be achieved because of the low effective sink temperature. A sample problem will be presented in appendix B to show the effect of location on radiator size.

Lunation effects on heat-rejection rates. - The effects of lunation on the heat-rejection capabilities of a radiator are shown in figure 4. The three cases discussed earlier (A, B, and C) are presented for the radiator surface temperatures given in table II (760° and 1460° R or 422 and 811 K). The values of α_s used in these calculations were for coatings chosen on the basis of compatability with the radiator surface temperature as indicated in table I. These values are indicated in the figure for each case. The radiators are located on the Moon's equator where the lunation effects are maximum.

Case A - horizontal position: One surface of the radiator is lying flat on the Moon and is thermally insulated from the lunar surface. The radiating surface cannot see the lunar surface, so that F_1 in equation (8) is zero as shown in table II.

Although the surface temperature of the Moon varies about 460° R (256 K) during a lunation, performance is not greatly affected because the radiator does not see the Moon. For a radiator surface temperature of 760° R (422 K), the heat flux emitted from the radiator is 514.6 Btu/(hr)(ft^2) (1.623 kW/m^2) (see table II). The solar radiation is zero at lunar sunrise and a maximum of 34.4 Btu/(hr)(ft^2) (0.108 kW/m^2) at lunar noon for $\alpha_s = 0.08$. Thus the net radiator heat flux is decreased to 480.2 Btu/(hr)(ft^2) (1.515 kW/m^2). This is a reduction of only about 7 percent. For $\alpha_s = 0.20$ the reduction increases to 17 percent.

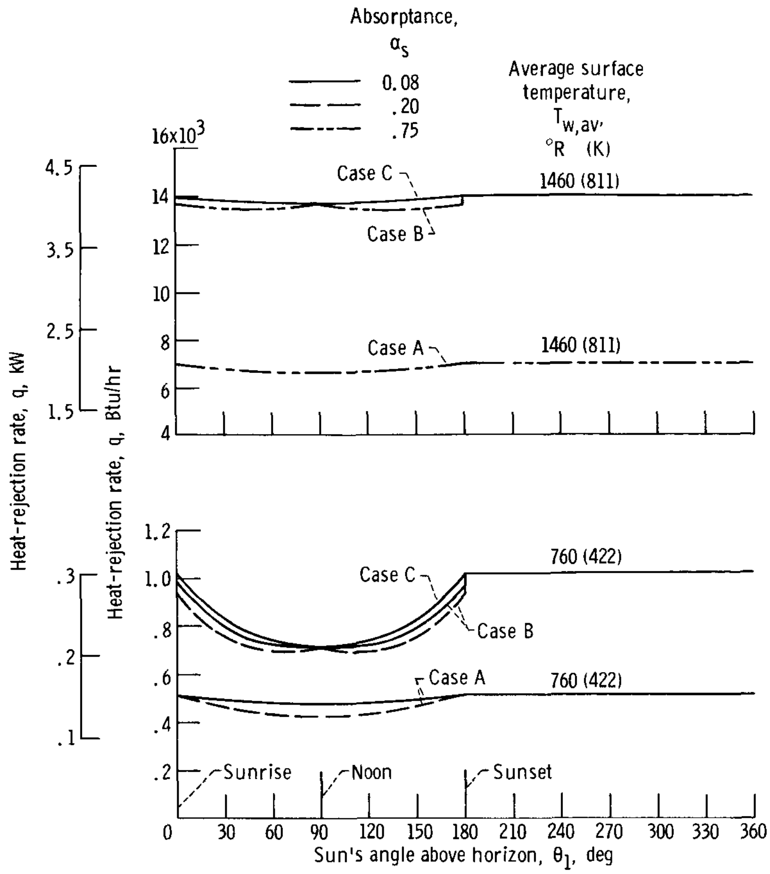

Figure 4. - Effects of Lunation on heat-rejection rate for high and low radiator temperatures. Heat-rejection rate given for 1- by 1-foot (0.305- by 0.305-m) section of radiator. Radiators located on equator. Emittance, 0.9. Only prime radiator surfaces considered.

The beneficial effects of increasing radiator wall temperatures for all three cases is clearly shown in figure 4 by the large increase in heat-rejection rate when increasing $T_{w,av}$ from 760° to 1460° R (422 to 811 K).

Case B - vertical position, solar energy incident: For this case the radiator is normal to the lunar surface, and both sides of the radiator are active. The plane of the radiator is normal to the plane of the ecliptic and is located on the equator. Since both sides of the surface are active, the maximum heat-rejection rate is higher than the horizontal case (case A) by about a factor of two for a comparable radiating temperature.

At the lower radiating temperature (760° R or 422 K) the heat-rejection rate varies by a factor of about 1.44 between lunar midday and night conditions. As the radiating temperature increases (1460° R or 811 K), the midday to night lunar effect decreases to 1.023. This decreasing effect is due to the surface emission of the radiator increasing by the fourth power of temperature while the contribution from the lunar surface and Sun remains unchanged. The effect on heat-rejection rate for different values of α_s is most apparent during lunar sunrise and sunet.

Case C - vertical position, no direct solar energy incident: For this case the radiator is also normal to the lunar surface and is located on the equator. The plane of the radiator is essentially in the plane of the ecliptic. Thus the direct solar energy is not incident on the surfaces of the radiator. Both sides of the radiator are active. The overall heat-rejection rates for this case are not very different from case B.

Comparison of Cases A, B, and C: Difference in heat-rejection rates for a range of radiator average wall temperatures considered for the three cases are shown in figure 5.

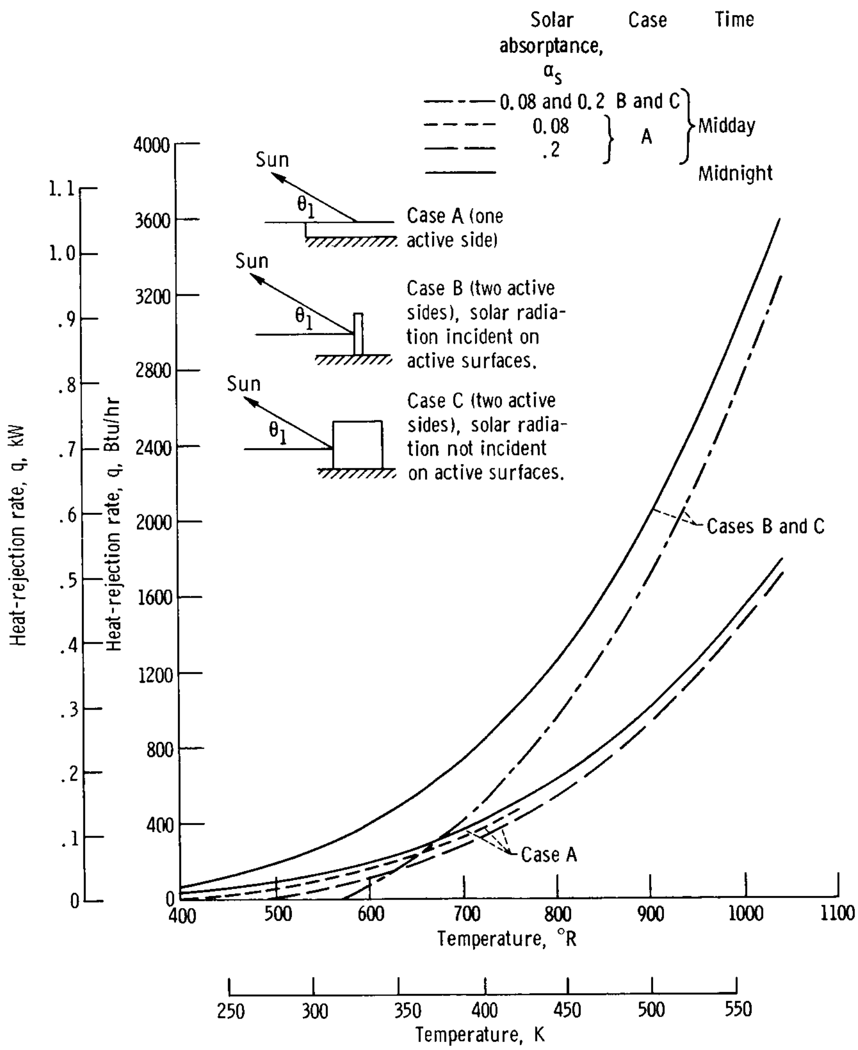

(a) $T_{w,av}$, 400° to 1040° R (222 to 578 K).

Figure 5. - Heat-rejection rate versus average surface temperature with radiator located on equator. Heat-rejection rate given for 1- by 1-foot (0.305- by 0.305-m) section of radiator. Only prime radiator surfaces considered.

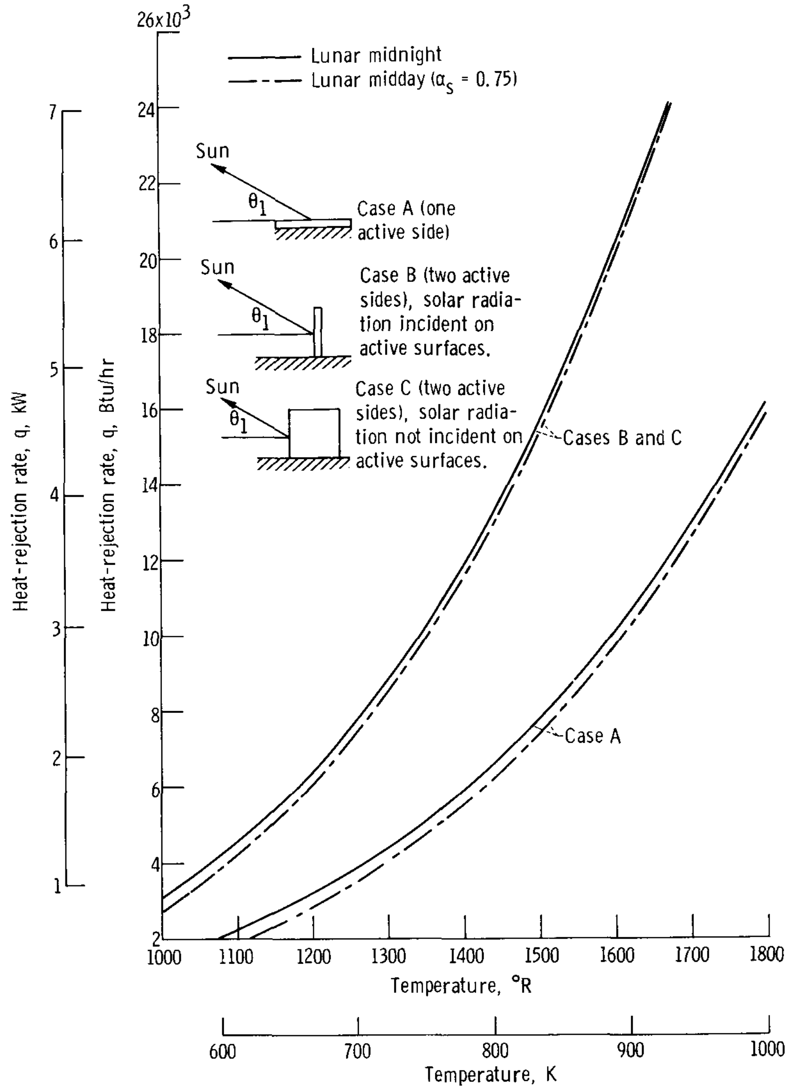

(b) $T_{w,av}$, 1000° to 1800° R (555.5 to 1000 K).

Figure 5. - Concluded.

The two specific time periods chosen are lunar high noon and midnight. Figure 5(a) covers $T_{w,av}$ from 400° to 1040° R (222 to 578 K) for $\alpha_s = 0.08$ and 0.20. Figure 5(b) covers $T_{w,av}$ from 1000° to 1800° R (555 to 1000 K) for the same times and $\alpha_s = 0.75$. As noted previously, the results for cases B and C fall on the same curve, and the heat-rejection rate for both cases is about twice the value for case A.

Little difference exists between noon and midnight heat-rejection rates for cases B and C until the design temperature of the radiator falls below 1000° R (555 K). Below this level, the heat-rejection rate for cases B and C during the nighttime period is appreciably higher than noontime.

The magnitude of the effect on heat-rejection rate with appropriate values of α_s between midday and midnight condition can be seen by the results presented in figure 6.

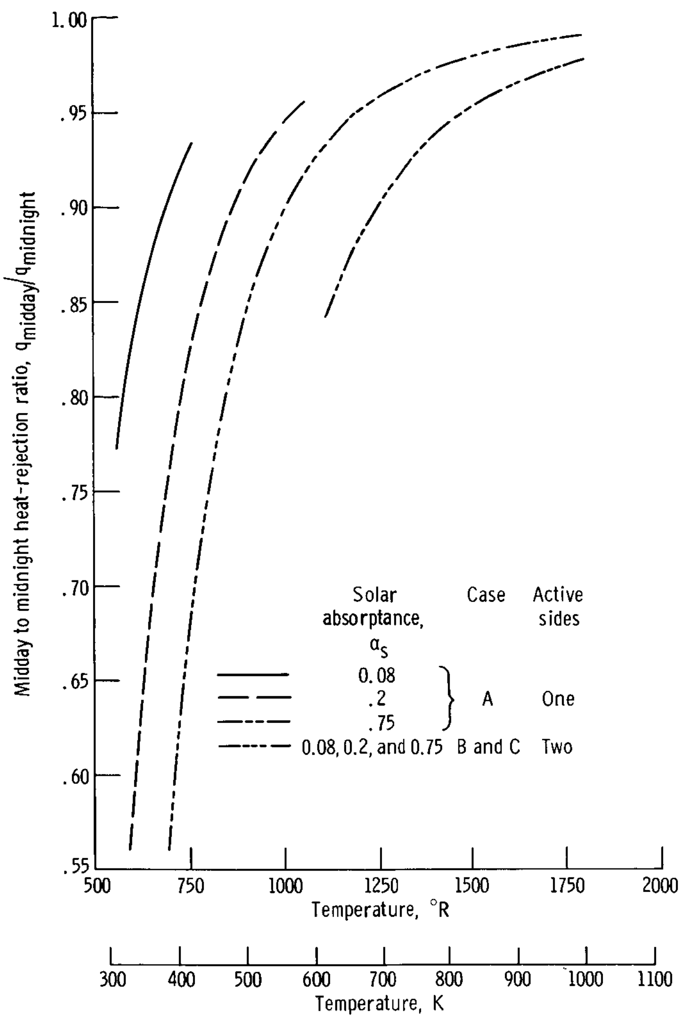

Figure 6. - Midday to midnight heat-rejection ratio versus average surface temperature for radiator located on equator.

In this figure the ratio of midday to midnight heat-rejection rate $q_{midday}/q_{midnight}$ is plotted against the average radiator temperature. The ratio is representative of the variation in performance of a heat-rejection system over a complete lunation at a specific radiator design temperature. All three radiators show less loss of heat-rejection capacity at midday as the radiator temperature increases. For low values of α_s, the horizontal radiator shows less loss than the vertical. If only coatings with high α_s are available, the horizontal radiator suffers greater degradation of capacity than the vertical ones.

Lunar Radiator Design Curves

The procedure used for calculating radiator heat-rejection rates in the performance section indicated the usefulness of design curves for radiator studies. Curves for the solutions of equations (6) or (7), which convert T_f to T_w, and for equation (20), which gives $T_{w,av}$, greatly simplified the computations. In addition, curves like those presented in figure 4 are essentially the solutions of equation (11) as the effective sink temperature varies during one lunation as shown in figure 3.

With three such sets of curves, it is threrfore possible to determine the heat-rejection capacity of a lunar radiator. Figures 7 and 8 present the curves for equations (6) or (7) and (20) for three different values of h_R. Figure 9 presents the solution curves for equation (11) for the three radiator configurations previously considered.

Briefly, the procedure for obtaining heat-rejection rates and radiator size using the design curves is as follows:

(1) For a given radiator inlet and outlet fluid temperature T_{fi} and T_{fo} find T_{wi} and T_{wo} using figure 7. Choose the value of h_R most likely to exist in the radiator for the fluid used. The sink temperature T_s can be found from figure 3 for each configuration at any time during the lunar day.

(2) With T_{wi} and T_{wo} find $T_{w,av}$ using figure 8. Use the same values for h_R and T_s as given previously.

(3) Knowing $T_{w,av}$, obtain q from figure 9 for the specified orientation, solar absorptance, and the desired lunar time.

(4) For a given radiator load Q (eq. (1)) and q (determined previously), the prime radiator area A_R can be found using equation (23) as shown in the section METHOD OF ANALYSIS:

$$A_R = \frac{Q}{q}$$

(5) When the actual radiator tube configuration is selected, the heat-transfer coefficient h_R should be checked against the assumed value of h_R for reasonable agreement. A detailed example using these curves will follow in appendix C.

If it becomes advantageous to use different coatings in different temperature regions of a radiator, the above procedure can be used treating the regions as separate radiators in series.

The values of the parameters used in generating these curves are compatible with the systems being considered for lunar application. The radiator average wall temperature ranges from 560° to 1660° R (311 to 922 K) to cover present-day Brayton or Rankine cycle system design. Emittance values of 0.70 and 0.90 were considered during the anal-

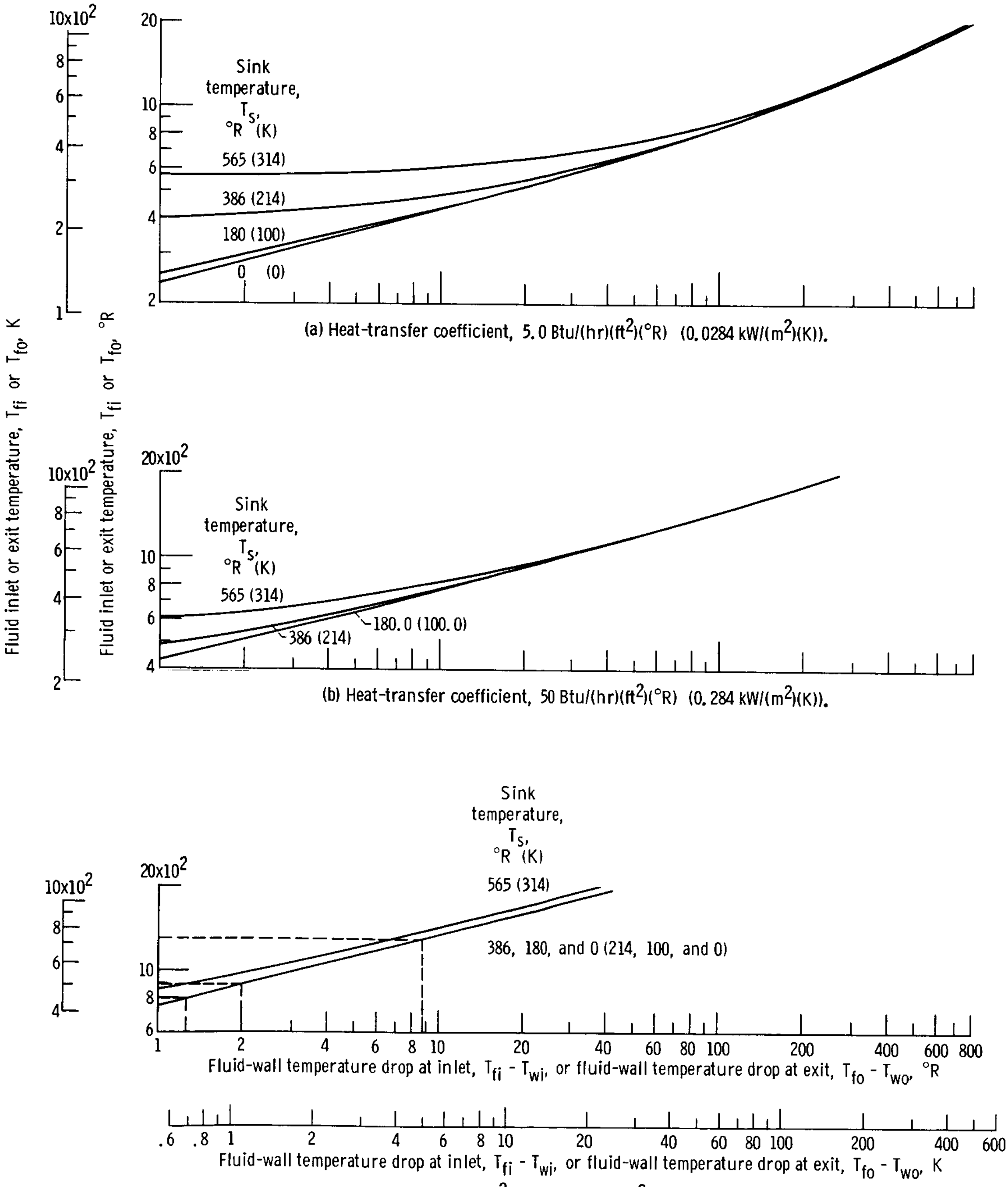

(c) Heat-transfer coefficient, 500 Btu/(hr)(ft^2)(°R) (2.84 kW/(m^2)(K)). Dashed lines for example in appendix B.

Figure 7. - Fluid temperature as function of temperature difference between fluid and wall. Emittance, 0.90.

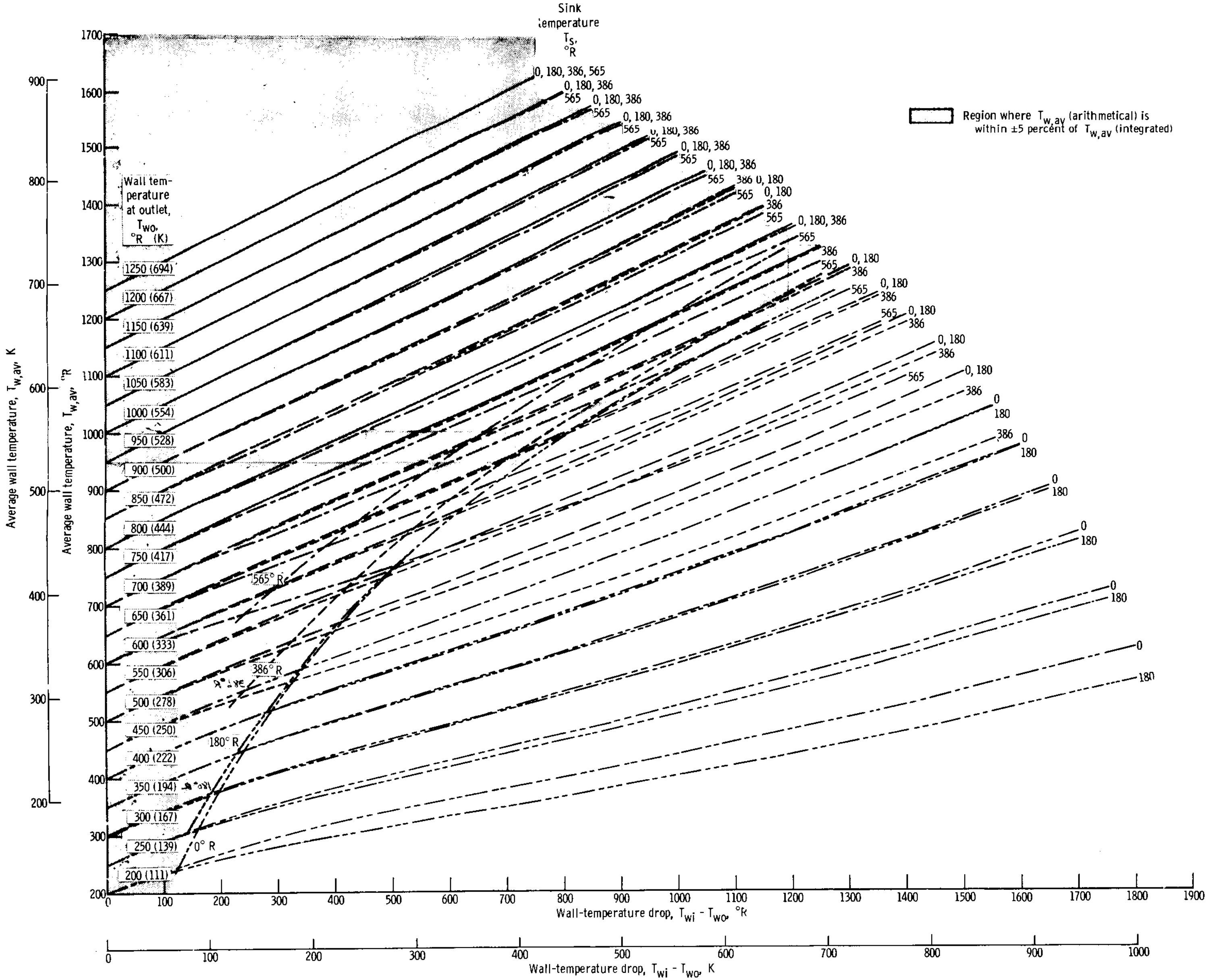

(a) Heat-transfer coefficient, 5 Btu/(hr)(ft^2)(°R) (0.0284 kW/(m^2)(K)). Emittance, 0.90.

Figure 8. - Average wall temperature as function of wall-temperature drop. (Sink temperature, 0°, 180°, 386°, and 565° R (0, 100, 214, and 565 K.)

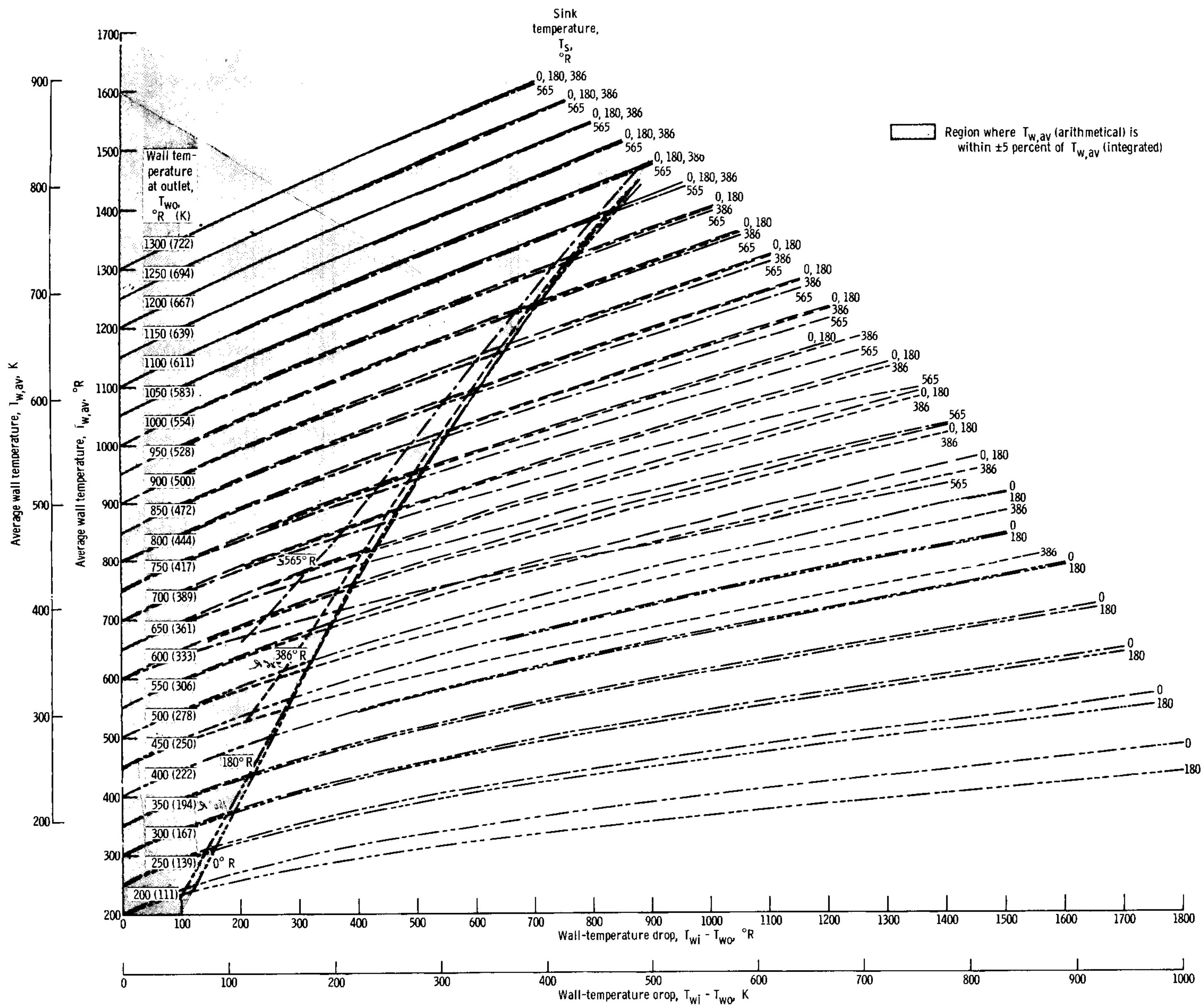

(b) Heat-transfer coefficient, 50 Btu/(hr)(ft^2)(°R) (0.284 kW/(m^2)(K)).

Figure 8. - Continued.

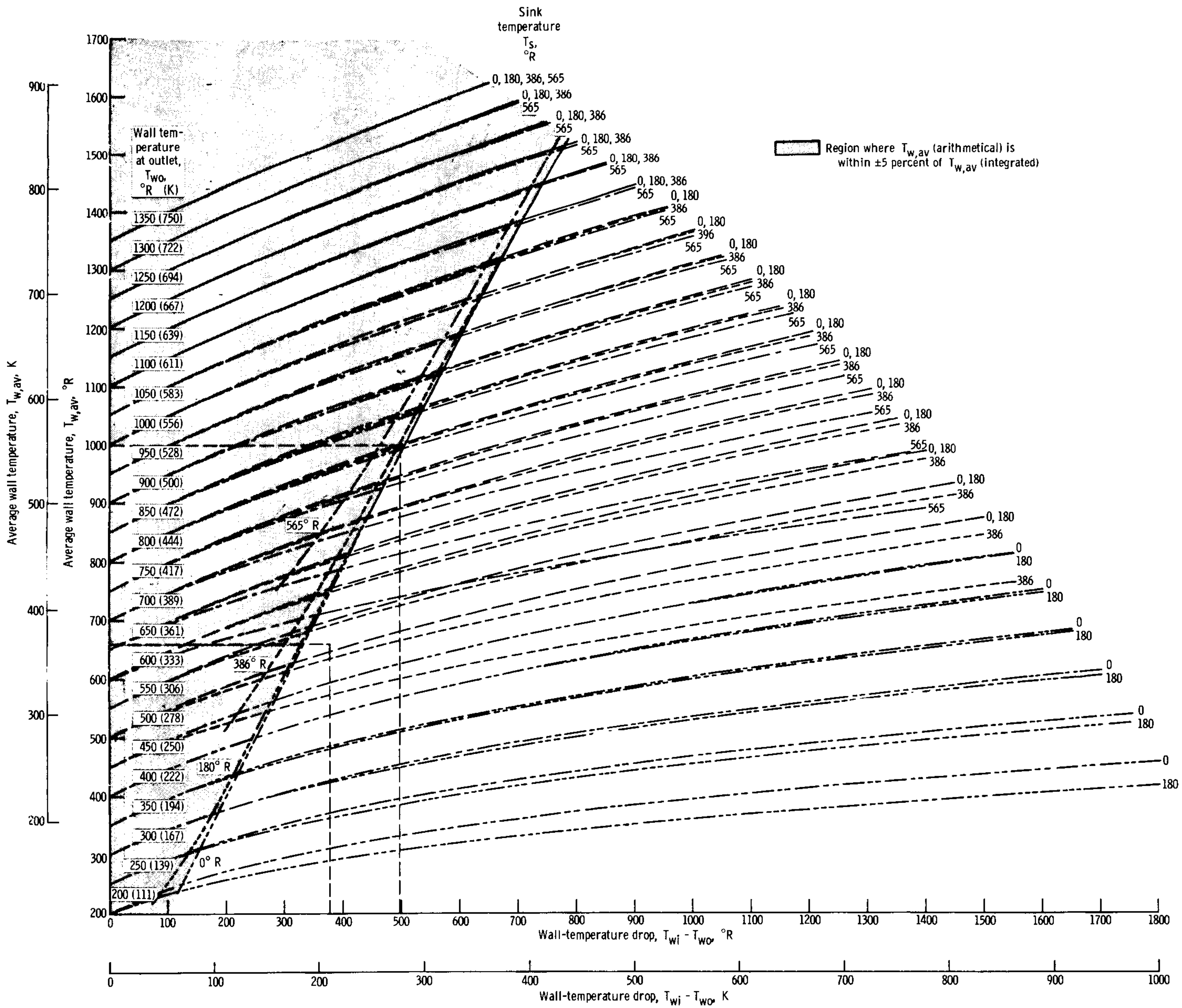

(c) Heat-transfer coefficient, 500 Btu/(hr)(ft^2)(°R) (2.84 kW/(m^2)(K)).

Figure 8. - Concluded.

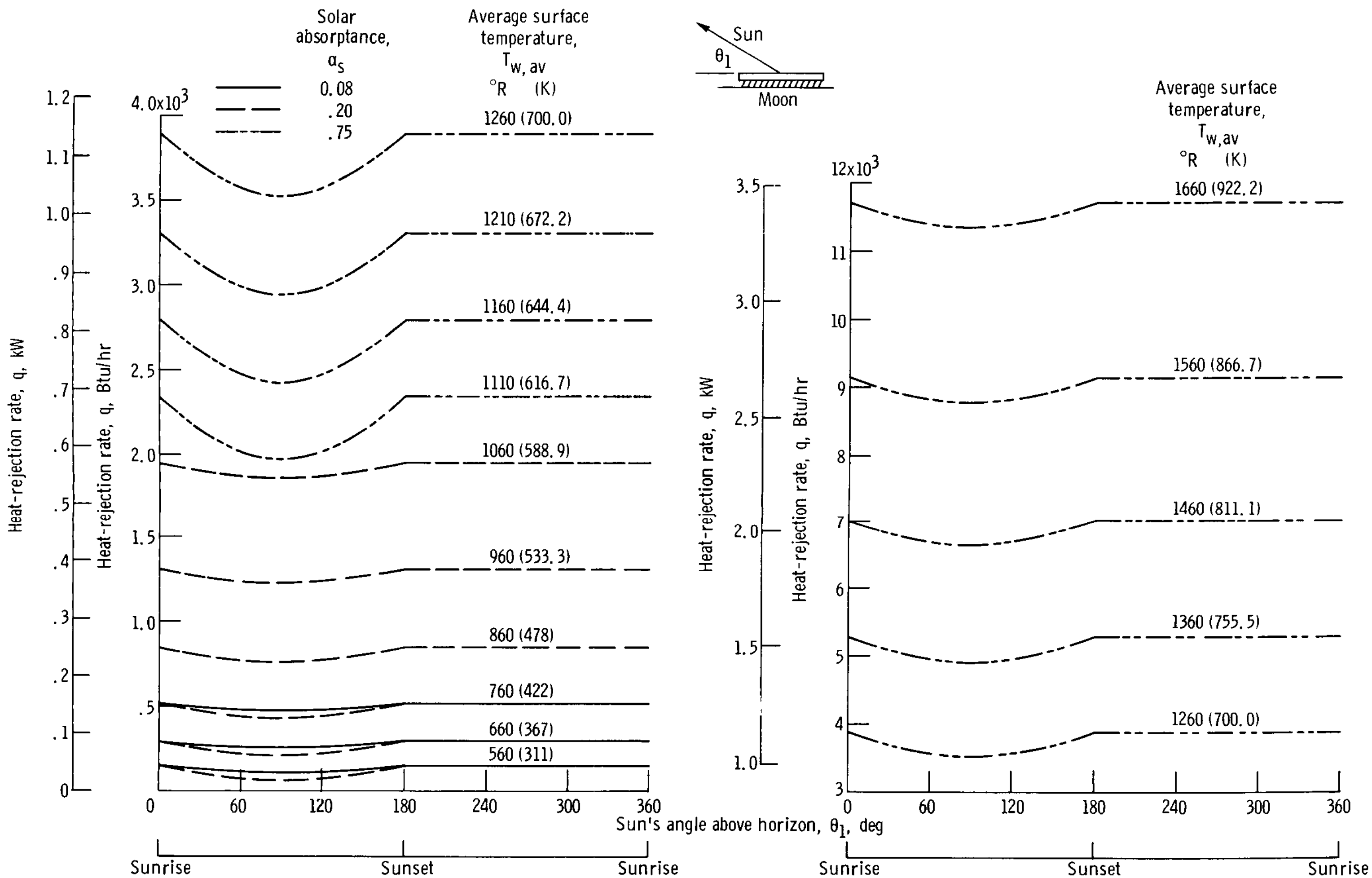

(a) Case A; one active side.

Figure 9. - Radiative heat-rejection rate versus Sun's angle for 1 lunar day with radiator located on equator. Emittance, 0.9; values of q given for 1- by 1-foot (0.305- by 0.305-m) section of radiator. Only prime radiator surfaces considered.

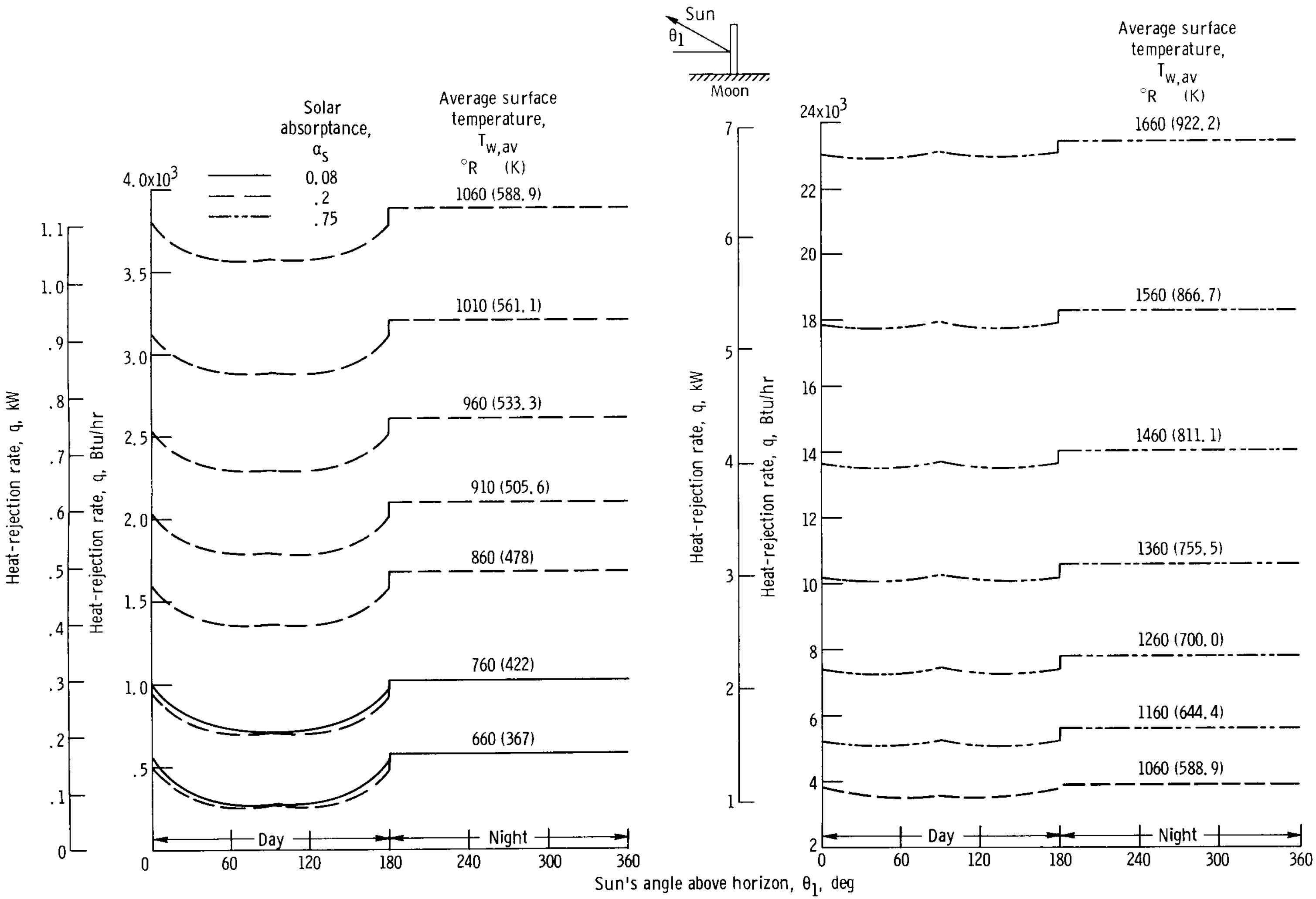

(b) Case B; two active sides. Solar radiation incident on active sides.

Figure 9. - Continued.

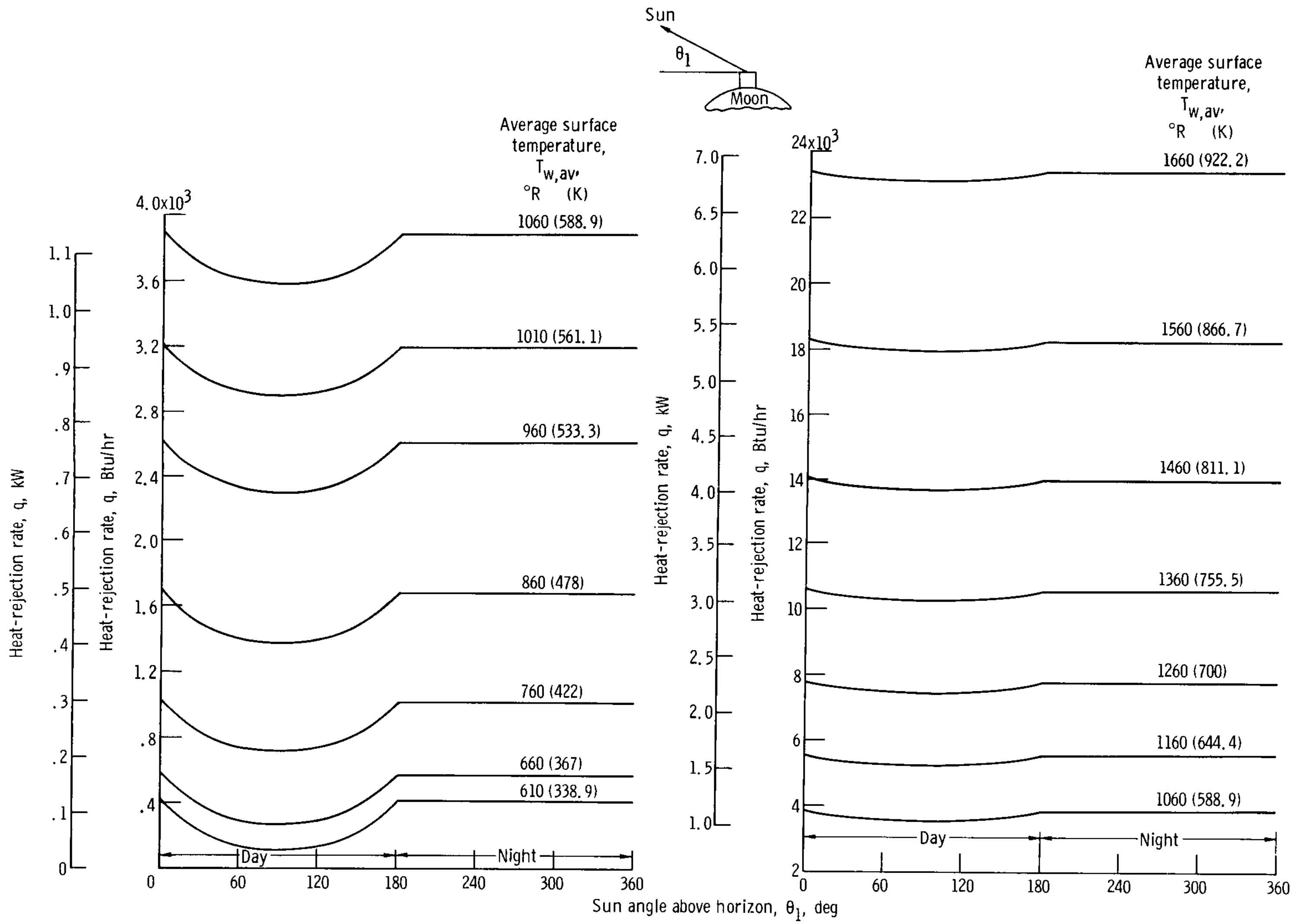

(c) Case C, two active sides. Solar radiation not incident on active surfaces.

Figure 9. - Concluded.

ysis. Since these two values made small changes in the results, only $\epsilon = 0.90$ is shown on these curves.

In the solutions of equations (6) or (7) and (20) (see figs. 7 and 8) three heat-transfer coefficients h_R were selected: 5, 50, and 500 Btu/(hr)(ft^2)(^{o}R) (0.0284, 0.284, and 2.84 kW/(m^2)(K)). It was determined that values greater than 500 Btu/(hr)(ft^2)(^{o}R) (2.84 kW/(m^2)(K)) had little effect on the results. A value of 500 Btu/(hr)(ft^2)(^{o}R) (2.840 kW/(m^2)(K)) is representative of a liquid-metal coolant system. The value of 5Btu/(hr)(ft^2)(^{o}R) (0.0284 kW/(m^2)(K)) is representative of a gas system, and 50 Btu/(hr)(ft^2)(^{o}R) (0.0284 kW/(m^2)(K)) is for an intermediate condition. The effective sink temperatures used for the curves cover the maximum and minimum values (lunar noon and midnight) for most of the conditions considered for the three radiator cases. For temperatures other than these interpolation is necessary.

The plots of the design curves show certain trends that may be helpful as guide lines in using these curves. The diminishing effect of the effective sink temperature T_s is shown in figure 7 as h_R increases from 5 to 500 Btu/(hr)(ft^2)(^{o}R) (0.0284 to 2.840 kW/(m^2)(K)).

In general, figure 8 shows at both high radiator outlet temperatures and small $(T_{wi} - T_{wo})$ the effect of T_s on $T_{w,av}$, is negligible. Included in this figure are shaded regions in which the values of $T_{w,av}$ obtained by using an arithmetic average are within 5 percent of the values obtained from equation (20). These regions are presented so that the user can make a quick judgment as to whether an arithmetic average will suffice rather than using equation (20) for points of interest falling away from the parametric values presented. Boundaries for these regions are basically the ordinate and the effective sink temperature. Four specific temperatures considered in the performance studies are shown as the outer boundaries for these regions.

CONCLUDING REMARKS

The equations and graphs in this report permit a rapid estimate of the effective sink temperature and of the size of a waste-heat-rejection radiator for a given lunar thermodynamic system whether for refrigeration, power generation, or component cooling. The analysis herein was limited to polar and equatorial locations and to one horizontal and two vertical attitudes (one in the plane of the ecliptic and one perpendicular to it). The results, however, provide good coverage because they are the extremes of limits.

The general conclusions are

1. A vertical radiator is better than a horizontal radiator, at least if its temperature is above 566^o R (314 K), because it has two active sides.

2. A polar location is better than an equatorial location.

3. High average radiator temperature is desirable from the standpoint of minimizing radiator size.

4. Direct solar radiation has little effect, since it appears that a properly selected coating (α_s/ϵ ratio) can match radiator average temperature.

A final choice of radiator geometry, location, and orientation will depend on many additional factors not herein considered: among them, weight of meteoroid protection, radiator structural weight, flexibility of location on lunar surfaces, more accurate accounting of the lunar radiation environment, and operational factors associated with lunar landing, transport, erection and maintenance.

More specific details follow:

5. Direct solar radiation can be made small by proper choice of a α_s/ϵ ratio that is compatable with the radiator average wall temperature, for example:

Radiator temperature		Solar absorptance, α_s	Emittance, ϵ	Ratio = Maximum solar heating / Heat emission		
$^{\circ}F$	K			Percent	Btu/(hr)(ft^2)	kW/m^2
760	422	0.08	0.9	6.7	$\frac{34.4}{514.6}$	$\frac{0.1082}{1.623}$
1460	811	0.75	0.9	4.6	$\frac{322.5}{7009.1}$	$\frac{1.015}{22.107}$

6. If an average radiator wall temperature lower than 566° R (314 K) is required, a horizontal radiator with an insulated back is necessary for daytime operation. The effective sink temperature at high noon on the lunar equator for a vertical radiator is 566° R (314 K). And for a horizontal radiator the effective sink temperature is 386° R (214 K) for an $\alpha_s = 0.08$ and 484° R (268 K) for $\alpha_s = 0.20$.

7. In the sample design problem in appendix C, a Brayton cycle powerplant operating in the polar region (sink temperature, $\approx 180^{\circ}$ R or 100 K) is compared with one operating at the equator at lunar midday (sink temperature, $\approx 565^{\circ}$ R or 314 K). The results indicate that a 23-percent reduction in radiator area can be achieved by using the polar location if constant power is required. It should be noted that, in a complete analysis, the effects of changes in efficiencies of other components in the system must be considered.

Lewis Research Center,
National Aeronautics and Space Administration,
Cleveland, Ohio, June 22, 1970,
120-27.

APPENDIX A

SYMBOLS

A_R prime radiator size[1], ft^2; m^2

A'_R prime radiator area, ft^2; m^2

a albedo

C_p specific heat of fluid, Btu/(lb)(^oR); J/(kg)(K)

D_a Earth days measured from lunar sunrise

F shape factor or view factor

G_s solar constant, 430 Btu/(hr)(ft^2); 1.356 kW/m^2

h_R convective heat-transfer coefficient based on outside radiating prime area, Btu/(hr)(ft^2)(^oR); kW/(m^2)(K)

I_n solar energy rate reflected per Moon unit area, Btu/(hr)(ft^2); kW/(m^2)

Q total heat-rejection flow rate, Btu/hr; kW

q heat-rejection flow rate for a 1- by 1-ft (0.305- by 0.305-m) section of radiator[1]

q_a solar albedo energy rate being absorbed by a 1- by 1-ft (0.305- by 0.305-m) section of vertical radiator, Btu/hr; kW

S entropy, Btu/(lb)(^oR); J/(kg)(K)

T temperature, ^oR; K

T_s effective sink temperature, ^oR; K

w fluid flow rate, lbm/hr; kg/hr

α_s solar absorptance

γ ratio of specific heats

ϵ emittance of radiator

η_{cy} Brayton cycle efficiency

θ_1 angle between Sun and horizontal radiating surface

θ_n angle between Sun and normal to radiating surface

σ Stefan-Boltzmann Constant, 0.17132×10^{-8} Btu/(hr)(ft^2)($^oR^4$); 5.6671×10^{-11} kW/(m^2)(K^4)

Subscripts:

a albedo

av integrated average

f fluid

i inlet

M Moon

o outlet

R radiator

rej rejection

w wall

1 active side of a radiator with one side insulated or one side of a radiator with two active sides

---

[1]Radiator may have one active side or two active sides; also only prime radiator area or size is considered.

2 second side of a radiator with two active sides

Superscript:

* Brayton cycle temperatures (see fig. 11)

' heat exchanger fluid temperatures, waste heat loop (see fig. 11)

APPENDIX B

THE MOON'S ALBEDO

For case A, the radiator is lying flat on the Moon, and the bottom is thermally insulated from the Moon's surface. Since the surface of the radiator does not see the surface of the Moon, there is no albedo heat flux incident on the radiator.

For the analysis of both cases B and C, the curvature of the lunar surface to be a plane. Also, it is commonly assumed that the planets and the Moon have diffusely reflecting surfaces which obey Lambert's Cosine Law (see ref. 11). Therefore, the shape or view factor (ref. 3) for a vertical radiator with two active sides will be 1.0 for both cases B and C.

The solar energy rate reflected per Moon unit area is given by the equation

$$I_r = G_s a \sin \theta_1 \tag{B1}$$

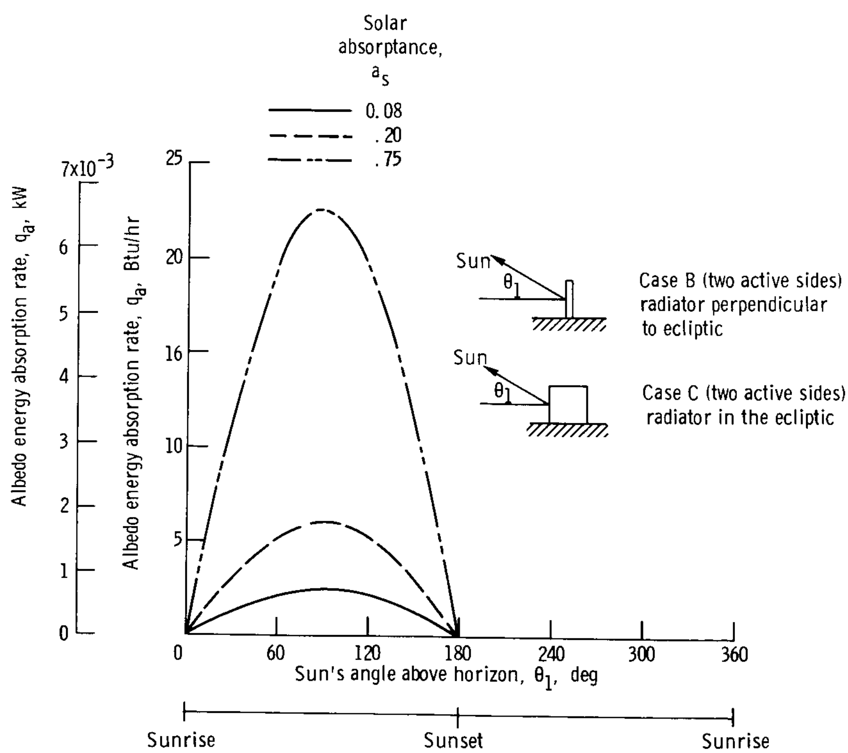

Figure 10. - Albedo energy absorption rate versus Sun's angle for 1 lunar day with radiator located at equator for cases B and C. Ordinate for a 1- by 1-foot (0.305- by 0.305-m) section of radiator.

The solar energy rate being absorbed by a 1- by 1-foot (0.305- by 0.305-m) section of vertical radiator is

$$q_a = F_a \alpha_s I_r = F_a \alpha_s G_s \, a \sin \theta_1 \tag{B2}$$

where F_a is 1.0 as stated albedo, G_s is 430 Btu/(hr)(ft^2) (1.356 kW/m^2), and the albedo a from reference 11 is 0.07. Figure 10 is a plot of the albedo energy absorption rate for the lunar daylight hours for a 1- by 1-foot (0.305- by 0.305-m) section of vertical radiator in which the several values of solar absorptance α_s used in the report are parameters. These curves can be used to make corrections to the data given in the report. However, from equation (B2), it is apparent that, even for the maximum albedo values, the energy rate incident upon the radiator is less than one tenth the value of the maximum direct energy rate from the Sun, and in most cases can be neglected.

APPENDIX C

SAMPLE PROBLEM USING DESIGN CURVES

To demonstrate the use of the curves two sample calculations will be performed. These calculations show how the radiator area is affected by the differences in sink temperature at the equator and at the poles of the Moon.

Two Brayton cycle power conversion systems are to be analyzed, both having the following conditions:

Alternator efficiency	0.90
Electrical power output, kW	500
Turbine inlet temperature, ^{o}R (K)	2060 (1144)
Turbine efficiency	0.850
Turbine-to-compressor pressure loss ratio	0.900
Recuperator effectiveness	0.900
Compressor efficiency	0.80

The combined temperature-entropy and flow diagram is shown in figure 11.

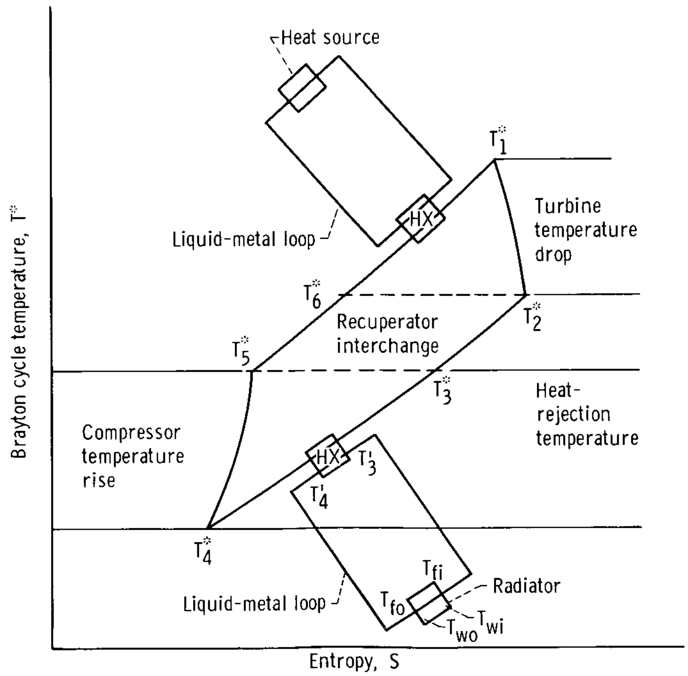

Figure 11. - Working temperatures for Brayton cycle power conversion system.

One system is located in the polar region with an effective sink temperature of approximately 180^{o} R (100 K), which is also approximately the nighttime sink temperature at the equator. The other is located at the equator with a maximum sink temperature of 565^{o} R (314 K) (lunar noon). In each case it is assumed that full-power operation is required throughout the lunar cycle. The systems will have a vertical radiator with two active sides. This configuration gives the maximum heat-rejection per unit area. An optimization procedure given in reference 1 will be used to obtain minimum radiator area for each case. The procedure involves plotting radiator areas against cycle temperature ratios for different turbine temperature ratios. Figures 7 to 9 will be used to obtain the radiator areas for these computations.

Because it is desirable to exclude the complication, the drop through the walls of the heat-rejection rate were also calculated. An example of this information is given Therefore,

$$T_3' = T_3^* = T_{fi}$$

and,

$$T_4' = T_4^* = T_{fo}$$

With the use of the equations given in reference 1, and with a γ (ratio of specific heats) of 1.67, the state points of the working fluid around the Brayton cycle were calculated for the various values of the parameters, cycle temperature ratio $(T_4/T_1)^*$, and turbine temperature ratio $(T_2/T_1)^*$. The thermodynamic cycle efficiency η_{cy} and the system heatrejection rate were also calculated. An example of this information is given in table III for the turbine temperature ratio $(T_2/T_1)^* = 0.75$.

The following table is abstracted from table III and shows, for the two values of $(T_4/T_1)^*$, the various derived values and the method of geeting them.

1	2		3		4		5		6		7		8		9	
Cycle temperature ratio, (T_4/T_1)	Source or derivation															
	From T_3 in table III and fig. 7(c) $(T_3 = T_{fi})$		From T_4 in table III and fig. 7(c) $(T_4 = T_{fo})$		Column 2 minus T_3 in table III		Column 3 minus T_4 in table III		Column 4 minus column 5		From fig. 8(c) using columns 5 and 6 and T_s		From column 7 and fig. 5(a)		Heat-rejection rate Q_{rej} divided by column 8	
	$T_{fi} - T_{wi}$		$T_{fo} - T_{wo}$		T_{wi}		T_{wo}		$T_{wi} - T_{wo}$		$T_{w,av}$		q		A_R	
	^{o}R	K	^{o}R	K	^{o}R	K	^{o}R	K	^{o}R	K	^{o}R	K	Btu/hr	kW	ft^2	m^2
0.25	2.0	1.1	<1	<0.51	893.0	496.1	515.0	286.0	378.0	210.1	660.0	366.7	582	0.171	5962	552.5
.39	8.8	4.9	1.25	.69	1300.2	722.3	801.8	445.3	498.4	277.0	1000.0	555.6	3080	.902	8858	824.0

TABLE III. - BRAYTON CYCLE RADIATOR AREA CALCULATION

[Brayton system power output, 500 kW_e; turbine inlet temperature, 2060° R (1144 K); sink temperature, 180° R (100 K); turbine temperature ratio, 0.75; recuperator effectiveness, 0.90; radiator heat-transfer coefficient, 500 Btu/(hr)(ft^2)($^{\circ}$R) (2.839 kW/(m^2)(K)).]

(a) U.S. Customary Units

Cycle temperature ratio, T_4/T_1	Brayton cycle temperatures, $^{\circ}$R (a)						Cycle efficiency, η_{cy}	Heat-rejection rate, Q_{rej}, Btu/hr	Fluid-wall temperature drop at inlet, $T_{fi} - T_{wi}$, $^{\circ}$R	Fluid-wall temperature drop at exit, $T_{fo} - T_{wo}$, $^{\circ}$R	Inlet wall temperature, T_{wi}, $^{\circ}$R	Exit wall temperature, T_{wo}, $^{\circ}$R	Inlet-exit wall temperature drop, $T_{wi} - T_{wo}$, $^{\circ}$R	Average wall temperature, $T_{w,av}$, $^{\circ}$R	Heat-rejection rate, q, Btu/hr	Prime radiator size A_R, ft^2
	T_1	T_2	T_3	T_4	T_5	T_6										
0.25	2060	1545	895	515	823	1473	0.353	3.47×10^6	2.0	0	893.0	515.0	378.0	660	582	5 962
.26	↓	↓	924	536	856	1476	.334	3.779	2.2	↓	921.8	536.0	385.8	685	660	5 726
.27	↓	↓	954	556	888	1479	.315	4.127	2.5	↓	951.5	556.0	395.5	710	770	5 360
.28	↓	↓	984	577	921	1483	.295	4.525	2.9	↓	981.1	577.0	404.1	735	880	5 142
.29	↓	↓	1013	597	954	1486	.276	4.985	3.3	↓	1009.7	597.0	412.7	760	1026	4 859
.30	↓	↓	1043	618	987	1489	.256	5.522	3.6	↓	1039.4	618.0	421.4	785	1170	4 720
.31	↓	↓	1072	639	1020	1493	.235	6.158	4.0	↓	1068.0	639.0	429.0	810	1330	4 630
.32	↓	↓	1102	659	1053	1496	.215	6.924	4.4	↓	1097.6	659.0	438.6	835	1500	4 616
.33	↓	↓	1132	680	1086	1499	.194	7.862	4.8	↓	1127.2	680.0	447.2	855	1640	4 795
.34	↓	↓	1161	700	1119	1502	.173	9.040	5.4	↓	1155.6	700.0	455.6	880	1850	4 886
.35	↓	↓	1191	721	1152	1506	.152	10.560	6.0	↓	1185.0	721.0	464.0	905	2065	5 114
.36	↓	↓	1221	742	1185	1509	.131	12.600	6.6	↓	1214.4	742.0	472.4	930	2310	5 455
.37	↓	↓	1250	762	1217	1512	.109	15.480	7.2	1.00	1242.8	761.0	481.8	955	2560	6 047
.38	↓	↓	1280	783	1250	1516	.087	19.852	8.0	1.10	1272.0	781.9	490.1	980	2840	6 990
.39	↓	↓	1309	803	1283	1519	.065	27.283	8.8	1.25	1300.2	801.8	498.4	1000	3080	8 858
.40	↓	↓	1339	824	1316	1522	.043	42.712	9.8	1.40	1329.2	822.6	506.6	1025	3410	12 526

[a]See fig. 11 for identification of Brayton cycle temperatures.

TABLE III. - Concluded. BRAYTON CYCLE RADIATOR AREA CALCULATIONS

[Brayton system power output, 500 kW_e; turbine inlet temperature, 2060° R (1144 K); sink temperature, 180° R (100 K); turbine temperature ratio, 0.75; recuperator effectiveness, 0.90; radiator heat-transfer coefficient, 500 Btu/(hr)(ft^2)($^{\circ}$R) (2.839 kW/(m^2)(K)).]

(b) SI Units

Cycle temperature ratio, T_4/T_1	Brayton cycle temperatures, K (a)						Cycle efficiency, η_{cy}	Heat-rejection rate, Q_{rej}, kW	Fluid-wall temperature drop at inlet, $T_{fi} - T_{wi}$, K	Fluid-wall temperature drop at exit, $T_{fo} - T_{wo}$, K	Inlet wall temperature, T_{wi}, K	Exit wall temperature, T_{wo}, K	Inlet-exit wall temperature drop, $T_{wi} - T_{wo}$, K	Average wall temperature, $T_{w,av}$, K	Heat-rejection rate, q, kW	Prime size A_R, m^2
	T_1	T_2	T_3	T_4	T_5	T_6										
0.25	1144	858	497	286	457	818	0.353	1 017	1.1	0	496.1	286.0	210.1	366.7	0.171	552.5
.26			513	298	476	820	.334	1 107	1.2		512.0	298.0	214.0	380.6	.193	533.0
.27			530	309	493	822	.315	1 209	1.4		528.5	309.0	219.5	394.4	.226	497.2
.28			547	321	512	824	.295	1 326	1.6		545.0	321.0	224.0	408.3	.258	477.8
.29			563	332	530	825	.276	1 461	1.8		560.9	332.0	228.9	422.2	.300	455.0
.30			579	343	548	827	.256	1 618	2.0		577.4	343.0	234.4	436.1	.343	438.3
.31			596	355	567	829	.235	1 804	2.2		593.3	355.0	238.3	450.0	.390	430.0
.32			612	366	585	831	.215	2 029	2.4		609.7	366.0	243.7	463.9	.439	429.8
.33			629	378	603	833	.194	2 304	2.7		626.2	378.0	248.2	475.0	.481	445.0
.34			645	389	622	834	.173	2 649	3.0		641.9	389.0	252.9	488.9	.542	454.0
.35			662	401	640	837	.152	3 094	3.3		658.3	401.0	257.3	502.8	.605	475.2
.36			678	412	658	838	.131	3 692	3.7		674.9	412.0	262.9	516.7	.677	506.5
.37			694	423	676	840	.109	4 536	4.0	.56	690.4	422.4	268.0	530.6	.750	562.0
.38			711	435	694	842	.087	5 817	4.4	.61	706.6	434.4	272.2	544.4	.832	650.0
.39			727	446	713	844	.065	7 994	4.9	.69	722.3	445.3	277.0	555.6	.902	824.0
.40			744	458	731	845	.043	12 515	5.4	.78	738.4	457.2	281.2	569.4	.999	1165.0

[a] See fig. 11 for identification of Brayton cycle temperature.

The temperature drop between the liquid metal heat-rejection fluid and the radiator surface, for an assumed h_R of 500.0 Btu/(hr)(ft^2)(^{o}R) (2.840 kW/(m^2)(K)), is given in columns 2 and 3 for the inlet and outlet, respectively. As shown in column 2, the data are obtained from figure 7(c) (see the dashed lines); the argument or independent variable is T_3 or T_{fi}, which is the ordinate, and the temperature drop, $T_{fi} - T_{wi}$, is given by the abscissa. In a similar manner $T_{fo} - T_{wo}$ of column 3 is obtained in which T_4 or T_{fo} is used as the argument. All values less than 1^o R (0.156 K) are neglected.

As shown in columns 4 and 5, T_{wi} and T_{wo} are obtained by subtracting T_3 from column 2 and T_4 from column 3, respectively. Column 6, $T_{wi} - T_{wo}$, is simply the difference between columns 4 and 5.

The values for $T_{w,av}$ in column 7 are obtained from the ordinates of figure 8(c) (see the dashed lines in the figure) in which the parameters are T_s = 180^o R (100 K) and the wall outlet temperature T_{wo} (column 5). The argument (abscissa) is $T_{wi} - T_{wo}$, and the two values 378^o R (210.1 K) and 498.4^o R (277 K) are indicated by the dashed lines on figure 8(c) which lead to the two values of $T_{w,av}$ of 660^o R (366.7 K) and 1000^o R (555.6 K), respectively. For these values of $T_{w,av}$ (660^o and 1000^o R or 366.7 and 555.6 K) shown in column 8 the heat-rejection rates for a 1- by 1-foot (0.305- by 0.305-m) section of radiator per unit area q are 582.0 and 3080.0 Btu/hr (0.171 and 0.902 kW), respectively (from fig. 5(a)). Dividing the system heat-rejection rate Q_{rej} (table III) by q, the heat-rejection rate for a 1- by 1-foot (0.305- by 0.305-m) section, gives the prime radiator size A_R. These two points are illustrated in figure 12(a). In a similar manner the prime radiator area is calculated for other values of $(T_4/T_1)^*$ to generate the curve $(T_2/T_1)^*$ = 0.75 in figure 12(a). The entire procedure is repeated to produce curves for $(T_2/T_1)^*$ = 0.65 and 0.85. The results for a sink temperature of 565^o R (314 K) are given in figure 12(b).

The curves (figs. 12(a) and (b)) show that the optimum prime radiator for a sink temperature of 180^o R (100 K) is about 4600 square feet (410 m^2). For a sink temperature of 565^o R (314 K), the prime radiator area is about 6000 square feet (558 m^2). These results are indicative of what can be expected at different lunar locations. However, many other system problems would have to be considered before a powerplant is positioned in the polar regions solely for the reduction of radiator size.

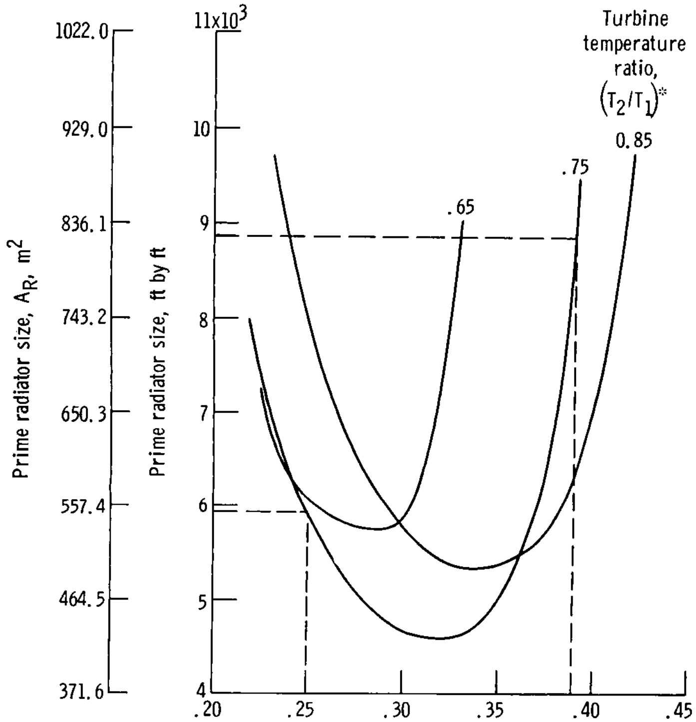

(a) Sink temperature, 180° R (100 K).

Figure 12. - Optimum cycle temperatures for minimum prime radiator size. Heat-transfer coefficient, 500 Btu per hour per square foot (0.284 W/(cm^2)(K)).

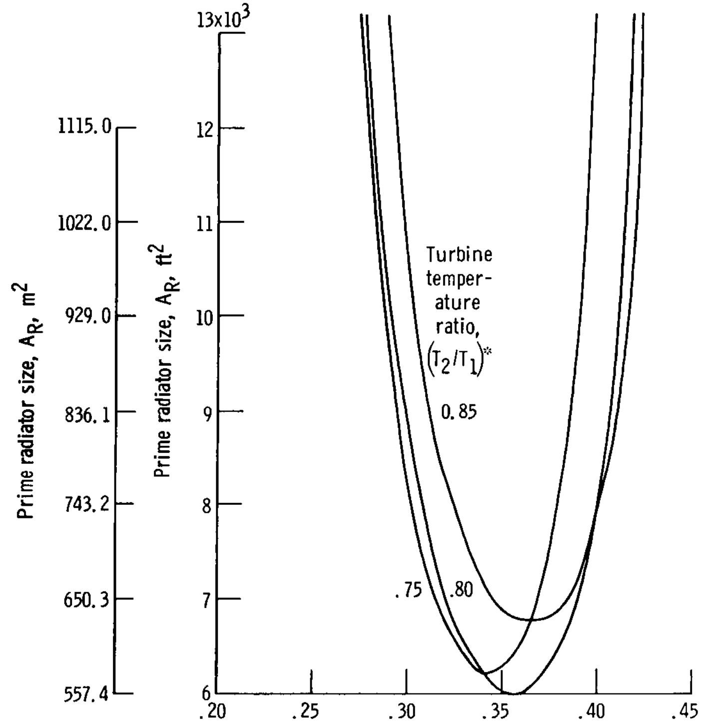

(b) Sink temperature, 565° R (314 K) (lunar midday).

Figure 12. - Concluded.

REFERENCES

1. Glassman, Arthur J.; and Stewart, Warner L.: A Look at the Thermodynamic Characteristics of Brayton Cycles for Space Power. Paper 63-218 AIAA, June 1963.

2. Mackay, Donald B.: Design of Space Powerplants. Prentice-Hall, Inc., 1963.

3. Hamilton, D. C.; and Morgan, W. R.: Radiant-Interchange Configuration Factors. NACA TN 2836, 1952.

4. Niedz, F. J.: Survey of the Physical and Environmental Parameters of the Moon. Rep. 4810, General Electric Co. (NASA CR-55064), Feb. 1963.

5. Stevenson, Jack A.; and Grafton, John C.: Lunar Temperature Environment. Proceedings of the 1969 National Meeting of the Institute of Environmental Sicences, Los Angeles, Apr. 6-8, 1960.

6. McAdams, William H.: Heat Transmission. Third Ed., McGraw-Hill Book Co., Inc., 1954, p. 63.

7. Grammer, J. R.; and Cunnington, G. R.: Emissivity Coatings for Low-Temperature Space Radiators. Rep. L-23-68-1, Lockheed Missles and Space Co., June 1968.

8. Crosby, J. R.: The development and Qualification of Thermal Control Coatings for SNAP Systems. Rep. NAA-SR-9908, Atomics International, Sept. 30, 1965.

9. Diedrich, James H.; and Curtis, Henry B.: Experimental Investigation of Total Emittance and Solar Absorptance of Several Coatings Between 300° and 575° K. NASA TN D-3381, 1966.

10. Cleary, R. E.; Emanuelson, R.; Luoma, W.; and Ammann, C.: Properties of High Emittance Materials. NASA CR-1278, 1969.

11. Ballinger, J.C.; Elizalde, J. C.; Garcia-Varela, R. M.; and Christensen, E. H.: Environmental Control Study of Space Vehicles. Part II: Thermal Environments of Space. Rep. ERR-AN-016, General Dynamics/Convair Astronautics, Nov. 1, 1960.

NASA-Langley, 1971 —— 33 E-4570